

1 Large fresh water influx induced salinity gradient and diagenetic 2 changes in the northern Indian Ocean dominate the stable oxygen 3 isotopic variation in *Globigerinoides ruber* 4

5 Rajeev Saraswat^{1*}, Thejasino Suokhrie¹, Dinesh K. Naik², Dharmendra P. Singh³, Syed M.
6 Saalim⁴, Mohd Salman^{1,5}, Gavendra Kumar^{1,5}, Sudhira R. Bhadra¹, Mahyar Mohtadi⁶, Sujata R.
7 Kurtarkar¹, Abhayanand S. Maurya³

8 ¹ Micropaleontology Laboratory, National Institute of Oceanography, Goa, India

9 ² Banaras Hindu University, Varanasi, Uttar Pradesh, India

10 ³ Indian Institute of Technology, Roorkee, India

11 ⁴ National Center for Polar and Ocean Research, Goa, India

12 ⁵ School of Earth, Ocean and Atmospheric Sciences, Goa University, Goa

13 ⁶ MARUM, University of Bremen, Bremen, Germany

14 * Correspondence to: Rajeev Saraswat (rsaraswat@nio.org)

15
16 **Abstract.** The application of stable oxygen isotopic ratio of surface dwelling planktic foraminifera *Globigerinoides*
17 *ruber* (white variety) ($\delta^{18}\text{O}_{ruber}$) to reconstruct past hydrological changes requires precise understanding of the effect
18 of ambient parameters on $\delta^{18}\text{O}_{ruber}$. The northern Indian Ocean, with huge freshwater influx and being a part of the
19 Indo-Pacific Warm Pool, provides a unique setting to understand the effect of both the salinity and temperature on
20 $\delta^{18}\text{O}_{ruber}$. Here, we use a total of 400 surface samples (252 from this work and 148 from previous studies), covering
21 the entire salinity end member region, to assess the effect of fresh water influx induced seawater salinity and
22 temperature on $\delta^{18}\text{O}_{ruber}$ in the northern Indian Ocean. The analyzed surface $\delta^{18}\text{O}_{ruber}$ very well mimics the expected
23 $\delta^{18}\text{O}$ calcite estimated from the modern seawater parameters (temperature, salinity and seawater $\delta^{18}\text{O}$). We report a
24 large diagenetic overprinting of $\delta^{18}\text{O}_{ruber}$ in the surface sediments with an increase of 0.18‰ per kilometer increase in
25 water depth. The fresh water influx induced salinity exerts the major control on $\delta^{18}\text{O}_{ruber}$ ($R^2 = 0.63$) in the northern
26 Indian Ocean, with an increase of 0.29‰ per unit increase in salinity. The relationship between temperature and
27 salinity corrected $\delta^{18}\text{O}_{ruber}$ ($\delta^{18}\text{O}_{ruber} - \delta^{18}\text{O}_{sw}$) in the northern Indian Ocean [$T = -0.59 * (\delta^{18}\text{O}_{ruber} - \delta^{18}\text{O}_{sw}) + 26.40$] is
28 different than reported previously, based on the global compilation of plankton tow $\delta^{18}\text{O}_{ruber}$ data. The revised
29 equations will help in better paleoclimatic reconstruction from the northern Indian Ocean by using the stable oxygen
30 isotopic ratio.

31

32 1. Introduction

33 The stable oxygen isotopic ratio ($\delta^{18}\text{O}$) of biogenic carbonates is one of the most extensively used marine paleoclimatic
34 proxies (Mulitza et al., 1997; Lea, 2014; Metcalfe et al., 2019; Saraswat et al., 2019). Even though it was initially
35 suggested that the oxygen isotopic fractionation in biogenic carbonates is largely driven by temperature (Urey et al.,
36 1947), subsequent work revealed that besides temperature, salinity and carbonate ion concentration of ambient
37 seawater also affects the biogenic carbonate $\delta^{18}\text{O}$ (Vergnaud-Grazzini, 1976; Spero et al., 1997; Bemis et al., 1998;
38 Spero et al., 1997; Bijma et al., 1999; Mulitza et al., 2003). On longer time-scales, the global ice volume contributes
39 the largest fraction ($\sim 1.0\text{-}1.2\%$) of the glacial-interglacial shift in marine biogenic carbonate $\delta^{18}\text{O}$, at a majority of the
40 locations (Shackleton, 1987; 2000; Lambeck et al., 2014). The ice volume changes have induced well-defined shifts
41 in biogenic carbonate $\delta^{18}\text{O}$ during the last several million years. Therefore, the regional evaporation-precipitation,
42 runoff and temperature changes are reconstructed from the global ice-volume corrected biogenic carbonate $\delta^{18}\text{O}$
43 (Wang et al., 1995; Kallel et al., 1997; Schmidt et al., 2004; Saraswat et al., 2012; 2013; Kessarkar et al., 2013).

44 The $\delta^{18}\text{O}$ of surface dwelling planktic foraminifera *Globigerinoides ruber* ($\delta^{18}\text{O}_{ruber}$) is often used to
45 reconstruct past surface seawater conditions (Saraswat et al., 2012; 2013; Mahesh and Banakar, 2014). Therefore,
46 continuous efforts are made to understand the factors affecting $\delta^{18}\text{O}_{ruber}$ (Vergnaud-Grazzini, 1976; Mulitza et al.,
47 1997; 2003; Waelbroeck et al., 2005; Mohtadi et al., 2011; Horikawa et al., 2015; Hollstein et al., 2017; Sanchez et al.,
48 2022). The depth habitat of *G. ruber* in the tropical Atlantic Ocean has been inferred from its stable oxygen isotopic
49 ratio (Farmer et al., 2007). The change in stable oxygen isotopic ratio of planktic foraminifera, including *G. ruber*, is
50 suggested as a proxy to reconstruct upper water column stratification in the tropical Atlantic Ocean, based on the good
51 correlation between $\delta^{18}\text{O}$ and the ambient seawater characteristics (Steph et al., 2009). A few studies suggested a
52 difference in the $\delta^{18}\text{O}$ of various morphotypes of *G. ruber* (sensu stricto and sensu lato) and attributed it to their distinct
53 ecology and depth habitat (Löwemark et al., 2005). However, a recent study from the Gulf of Mexico suggested a
54 similar ecology and depth habitat for both the *G. ruber* morphotypes (Thirumalai et al., 2014). The northern Indian
55 Ocean being influenced by huge fresh water influx as well as being a part of the Indo-Pacific Warm Pool (De Deckker,
56 2016), provides a unique setting to understand the effect of large salinity and temperature changes on $\delta^{18}\text{O}_{ruber}$. Earlier,
57 Duplessy et al., (1981) measured $\delta^{18}\text{O}$ of the living *G. ruber* specimens collected from the water column as well as of
58 the dead ones recovered from surface sediments of the northern Indian Ocean. A similar study from the Red Sea and
59 adjoining western Arabian Sea suggested that *G. ruber* calcifies its test in isotopic equilibrium with the ambient
60 seawater, thus tracking the inter-annual subtle change in the salinity and temperature (Kroon and Ganssen, 1989;
61 Ganssen and Kroon, 1991).

62 The temperature influence on $\delta^{18}\text{O}_{ruber}$ is well defined (Mulitza et al., 2003). The effect of fresh water influx
63 induced changes in ambient salinity on $\delta^{18}\text{O}_{ruber}$ is, however, debated (Dämmer et al., 2020). With the extensive use
64 of $\delta^{18}\text{O}_{ruber}$ to reconstruct regional evaporation-precipitation changes, especially from the monsoon dominated tropical
65 oceans, it is imperative to understand the precise influence of ambient salinity on $\delta^{18}\text{O}_{ruber}$. The ambient seawater pH,
66 carbonate ion concentration (Bijma et al., 1999), presence/absence of symbionts (Jørgensen et al., 1985) also affect
67 the isotopic composition of *G. ruber*. However, a limited glacial-interglacial variability in these parameters is masked

68 by the dominance of temperature and fresh water influx induced salinity changes in the oxygen isotopic ratio of *G.*
69 *ruber*. Additionally, the diagenetic changes, especially dissolution, also substantially alters the original isotopic
70 composition of the foraminifera shells (Berger and Killingley, 1977; Wu and Berger, 1989; Lohmann, 1995; McCorkle
71 et al., 1997; Wycech et al., 2018). The dissolution preferentially removes lighter oxygen rich sections of the shells,
72 thus increasing the whole shell $\delta^{18}\text{O}_{ruber}$ (Berger and Gardner, 1975; Lohmann, 1995; Weinkauff et al., 2020). The
73 studies based on the comparison of ambient parameters with the isotopic composition of living specimens collected
74 in plankton tows may not address the complete range of the changes in the isotopic signatures during the sinking of
75 the tests from the surface waters post death, and its subsequent deposition in the sediments at the bottom of the sea.
76 As the fossil shells are the sole basis to find out the isotopic ratio of the ambient seawater in the past, the effect of
77 diagenetic changes including the dissolution on foraminifer's oxygen isotopic ratio has to be properly evaluated. Here,
78 we assess the influence of fresh water influx induced strong salinity gradient, ambient temperature, depth induced
79 dissolution and other associated parameters on the stable oxygen isotopic ratio of the surface dwelling planktic
80 foraminifera *G. ruber* (white variety) in the surface sediments of the northern Indian Ocean.

81

82 **2. Ecology of *Globigerinoides ruber* (white)**

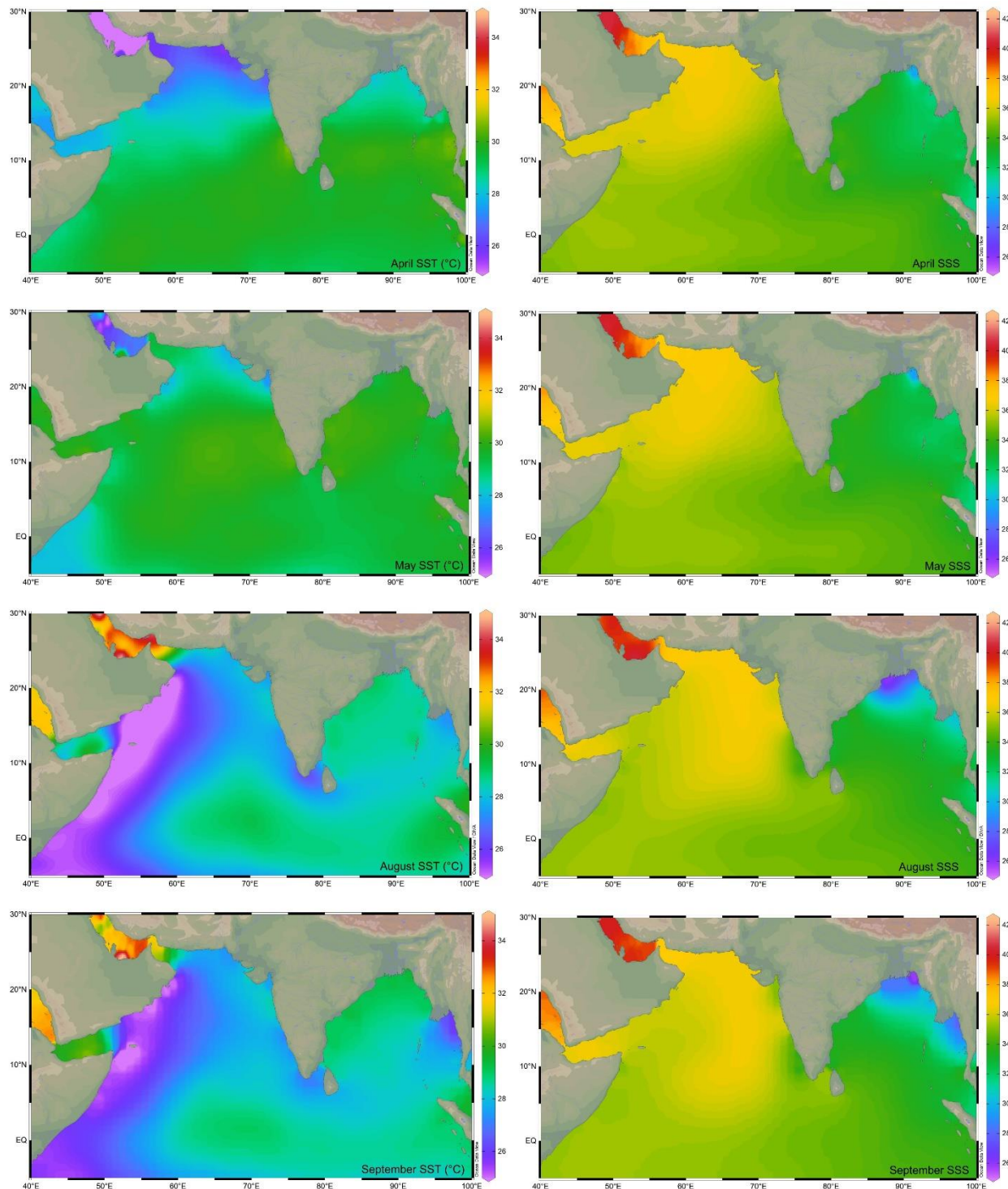
83 *Globigerinoides ruber* is a spinose planktic foraminifera inhabiting the mixed layer waters, throughout the year, in the
84 tropical-subtropical regions (Guptha et al., 1997; Kemle-von-Mücke and Hemleben, 1999). It is one of the dominant
85 planktic foraminifera in the northern Indian Ocean (Bé and Hutson, 1977; Bhadra and Saraswat, 2021) with its relative
86 abundance being as high as ~60% (Fraile et al., 2008). Its test is medium to low trochospiral and hosts algal symbionts
87 (Hemleben et al., 1989). *Globigerinoides ruber* prefers to feed upon phytoplankton (Hemleben et al., 1989), and is
88 dominant in oligotrophic warmer water with optimal temperature being 23.5°C (Fraile et al., 2008). However, it is
89 amongst a few planktic foraminifera species that can tolerate a wide range of salinity (22-49 psu) and temperature
90 (14-31°C) (Hemleben et al., 1989; Guptha et al., 1997). Two varieties of *G. ruber*, namely the white and pink are
91 common in the world oceans. However, the pink variety of *G. ruber* became extinct in the Indian and Pacific Oceans
92 at ~120 kyr during the Marine Isotopic Stage 5e (Thompson et al., 1979).

93

94 **3. Northern Indian Ocean**

95 The Indian Ocean with its northern boundary in the tropics includes two hydrographically contrasting basins, namely
96 the Arabian Sea and Bay of Bengal (BoB) (Figure 1). The excess of evaporation over precipitation generates high
97 salinity water mass that spreads throughout the surface of the northern Arabian Sea with its core as deep as ~100 m
98 (Shetye et al., 1994; Prasanna Kumar and Prasad, 1999; Joseph and Freeland, 2005). Other high salinity water masses
99 from both the Persian Gulf and Red Sea enter the northern Arabian Sea at deeper depths between 200-400 m and 500-
100 800 m, respectively (Rochford, 1964). A strong upwelling along the western boundary of the Arabian Sea during the

101 summer monsoon season brings cold, nutrient rich subsurface waters to the surface (Chatterjee et al., 2019). The weak
102 upwelling during the same season is also reported in the southeastern Arabian Sea (Smitha et al., 2014).



103
104 **Figure 1: The sea surface temperature (SST) (°C) (Locarnini et al., 2018) and salinity (SSS) (psu) (Zweng et al., 2018) in the**
105 **northern Indian Ocean during the monsoon (August-September) and non-monsoon (April-May) months. The major rivers**

106 **draining into the northern Indian Ocean, are marked by thin blue lines. The map has been prepared by using Ocean Data**
107 **View software (Schlitzer, 2018).**

108
109 The surface water is relatively fresher in the BoB, as the majority of the rivers from the Indian sub-continent
110 drain here, with the total annual continental runoff accounting to 2950 km³ (Sengupta et al., 2006). Additionally, the
111 total annual precipitation over the BoB is 4700 km³, and the evaporation is 3600 km³ (Sengupta et al., 2006). The high
112 salinity Arabian Sea water is transported into the BoB and the fresher BoB water mixes with the high salinity Arabian
113 Sea water, by the seasonally reversing coastal currents (Shankar et al., 2002). The upwelling during summer is
114 restricted to only the northwestern part of the BoB (Shetye et al., 1991). The upwelling combined with the convective
115 mixing during the winter season in the north-eastern Arabian Sea (Madhupratap et al., 1996) as well as eddies in the
116 BoB (Prasanna Kumar et al., 2004; Sarma et al., 2020) result in very high primary productivity in both the basins
117 (Qasim, 1977; Prasanna Kumar et al., 2009). The high primary productivity and fresh water capping induce strong
118 stratification and restricted circulation, that creates oxygen deficient zones (ODZ) at the intermediate depth in both
119 the Arabian Sea (Rixen et al., 2020; Naqvi, 2021) and BoB (Bristow et al., 2016, Sridevi and Sarma, 2020). The
120 Arabian Sea ODZ, however, is comparatively thicker and intense, leading to denitrification (Naqvi et al., 2006), which
121 is not reported yet from the BoB (Bristow et al., 2016).

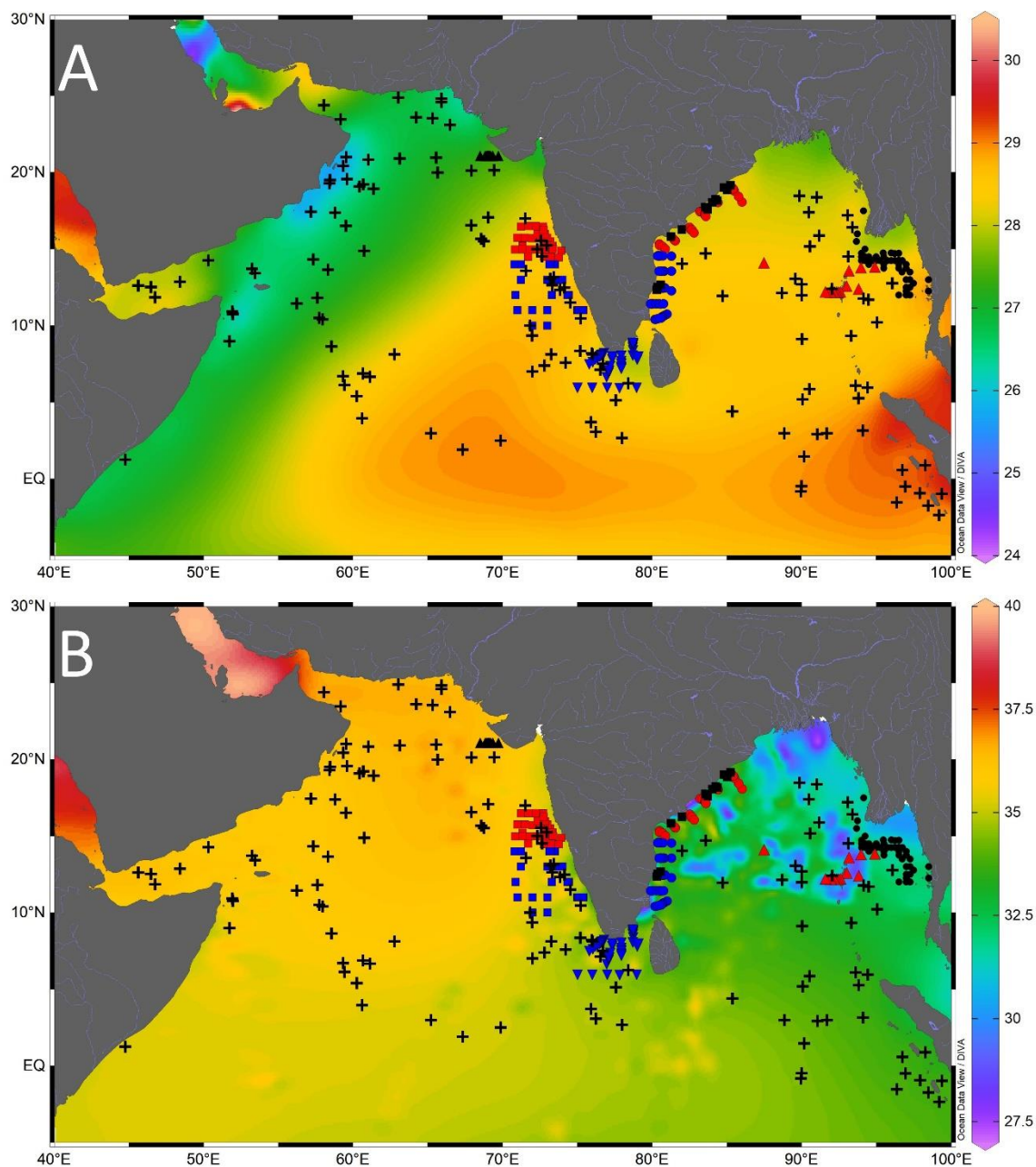
122 The equatorial Indian Ocean forms a part of the Indo-Pacific Warm Pool with the sea surface temperature
123 >28 °C throughout the year (Vinayachandran and Shetye, 1991; De Deckker, 2016). The marginal regions of the BoB
124 are comparatively warmer due to the fresh water influx from the rivers. The riverine influx shoals the mixed layer and
125 thickens the barrier layer, a buoyant layer separating the thermocline from the pycnocline, in the BoB (Howden and
126 Murtugudde, 2001). The riverine influx flows as a low salinity tongue all along the eastern margin of India (Chaitanya
127 et al., 2014). The annual average sea surface salinity (SSS) is <34 psu throughout the BoB, increasing from the head
128 bay towards south. In contrast to that, SSS remains >35 psu almost throughout the year in the Arabian Sea (Rao and
129 Sivakumar, 2003). The excess of evaporation over precipitation due to the dry northeasterly winds leads to the highest
130 salinity in the northern BoB during the winter (Rao and Sivakumar, 2003).

131

132 **4. Materials and Methodology**

133 The surface sediments were collected all along the path of the seasonal coastal currents in the northern Indian Ocean
134 (Figure 2, Supplementary Table 1). The samples from the Ayeyarwady Delta Shelf in the northeastern BoB were
135 collected during ‘India–Myanmar Joint Oceanographic Studies’ onboard Ocean Research Vessel *Sagar Kanya*
136 (SK175). A total of 110 surface sediment samples were collected from the water depths ranging from 10 m to 1080
137 m, on the Ayeyarwady Delta Shelf (Ramaswamy et al., 2008). The multicore samples were also collected at regular
138 intervals in transects running perpendicular to the coast, from the western BoB during the cruise SK308, onboard
139 Research Vessel *Sindhu Sadhana* (cruise SSD067) and Research Vessel *Sindhu Sankalp* (cruise SSK35). A total of
140 84 surface samples (including 71 multicore samples and 13 grab samples from sandy sediments) were collected from

141 the inner shelf to outer slope region of the eastern margin of India during the cruise SK308 (Suokhrie et al., 2021a;
142 Saalim et al., 2022). These samples from the western BoB represent the lowest salinity region in the northern Indian
143 Ocean (Panchang and Nigam, 2012). The multicore samples collected between 25 m and 2980 m in the Gulf of Mannar
144 and the region west of it (43 samples onboard Research Vessel *Sindhu Sadhana* SSD004) represent the zone of cross-
145 basin exchange of seawater between the BoB and the Arabian Sea (Singh et al., 2021). The spade core samples
146 collected from the southeastern Arabian Sea (ORV *Sagar Kanya* cruise SK117 and SK237) are located close to the
147 distal end of the low salinity BoB water intruding into the Arabian Sea. The multicore samples (13 number) collected
148 during SSD055 cruise, from the northeastern Arabian Sea, represent the warm saline conditions. We also collected
149 spade core surface samples from the Andaman Sea, onboard Research Vessel *Sindhu Sankalp* (cruise SSK98). A total
150 of 252 samples had sufficient *G. ruber* for isotopic analysis (Table 1). The new data was augmented with 148
151 previously published core-top studies (e.g. Sirocko, 1989; Prell and Curry, 1981; Duplessy et al., 1981; 1982) mainly
152 compiled by Waelbroeck et al., (2005). Therefore, a total of 400 surface sample data points were used for this study.



153
 154
 155
 156
 157
 158
 159
 160
 161

Figure 2: Location of the core top samples analyzed in this study (black filled triangle - cruise SSD055, red filled square - cruise SK117, blue filled square - cruise SK237, blue filled inverted triangle - cruise SSD004, blue filled circle - cruise SSD067, red filled circle - cruise SK308, black filled square - cruise SSK035, red filled triangle - cruise SSK098, black filled circle - cruise SK175), and the previously published core top values (black plus) compiled from the northern Indian Ocean. The background contours are temperature ($^{\circ}\text{C}$) (A) and salinity (psu) (B) with the scale on the right. Major rivers draining into the northern Indian Ocean, are marked by thin blue lines. The map was prepared by using Ocean Data View software (Schlitzer, 2018).

162

163 **Table 1: Details of the timing, region and the number of surface sediment samples collected in each expedition, used in this**
 164 **study (SK- Sagar Kanya, SSD- Sindhu Sadhana, SSK- Sindhu Sankalp).**

Sr.No.	Cruise	Month/Year	Area	Total Samples
1.	SK117	September-October 1996	Eastern Arabian Sea	27
2.	SK175	April-May 2002	North-eastern Bay of Bengal	45
3.	SK237	August 2007	South-eastern Arabian Sea	26
4.	SK308	January 2014	Northwestern Bay of Bengal	29
5.	SSD004	October-November 2014	Gulf of Mannar, Lakshadweep Sea	41
6.	SSD055	August 2018	North-eastern Arabian Sea	11
7.	SSD067	November-December 2019	South-western Bay of Bengal, Lakshadweep Sea, Eastern Arabian Sea	45
8.	SSK035	May-June 2012	Western Bay of Bengal	13
9.	SSK098	January-February 2017	Andaman Sea	15

165
 166 The surface sediment samples (0-1 cm) were processed following the standard procedure (Suokhrie et al.,
 167 2021b). The freeze-dried sediments were weighed and wet sieved by using 63 μm sieve. The coarse fraction ($>63 \mu\text{m}$)
 168 was dry sieved by using 250 μm and 355 μm sieves. For $\delta^{18}\text{O}$ analysis, 10-15 well preserved shells of *G. ruber* white
 169 variety were picked from 250-355 μm size range. We picked *G. ruber* s.s. wherever sufficient specimens were
 170 available. Unfortunately, several samples yielded very small carbonate fraction. In such samples, we picked mixed
 171 population of *G. ruber* to get sufficient specimens for isotopic analysis. The $\delta^{18}\text{O}_{ruber}$ was measured by using Finnigan
 172 MAT 253 isotope ratio mass spectrometer, coupled with Kiel IV automated carbonate preparation device. The samples
 173 were analyzed in the Alfred Wegner Institute for Polar and Marine Research, Bremerhaven, MARUM, University of
 174 Bremen, Bremen, Germany and the Stable Isotope Laboratory (SIL) at Indian Institute of Technology, Roorkee, India.
 175 The reference material 'National Bureau of Standards' (NBS 18/19) limestone was used as the calibration material
 176 and a secondary in-house standard was run after every 5 samples to detect and correct the drift. The precision of
 177 oxygen isotope measurements was better than 0.08‰. The $\delta^{18}\text{O}_{ruber}$ data generated on the newly collected surface
 178 sediments was augmented with the published core-top $\delta^{18}\text{O}$ measurements in the northern Indian Ocean. A total of
 179 400 surface sediment data points (252 from this work and 148 from the previous studies) were used to understand the
 180 factors affecting $\delta^{18}\text{O}_{ruber}$ in the northern Indian Ocean (Supplementary Table 1). The annual average sea surface
 181 temperature and salinity of the top 30 m water column at the respective sample locations was downloaded from the
 182 World Ocean Atlas (Boyer et al., 2013). The salinity and temperature at the core location was extrapolated from the
 183 nearby grid points, using the Live Access Server at the National Institute of Oceanography, Goa, India.

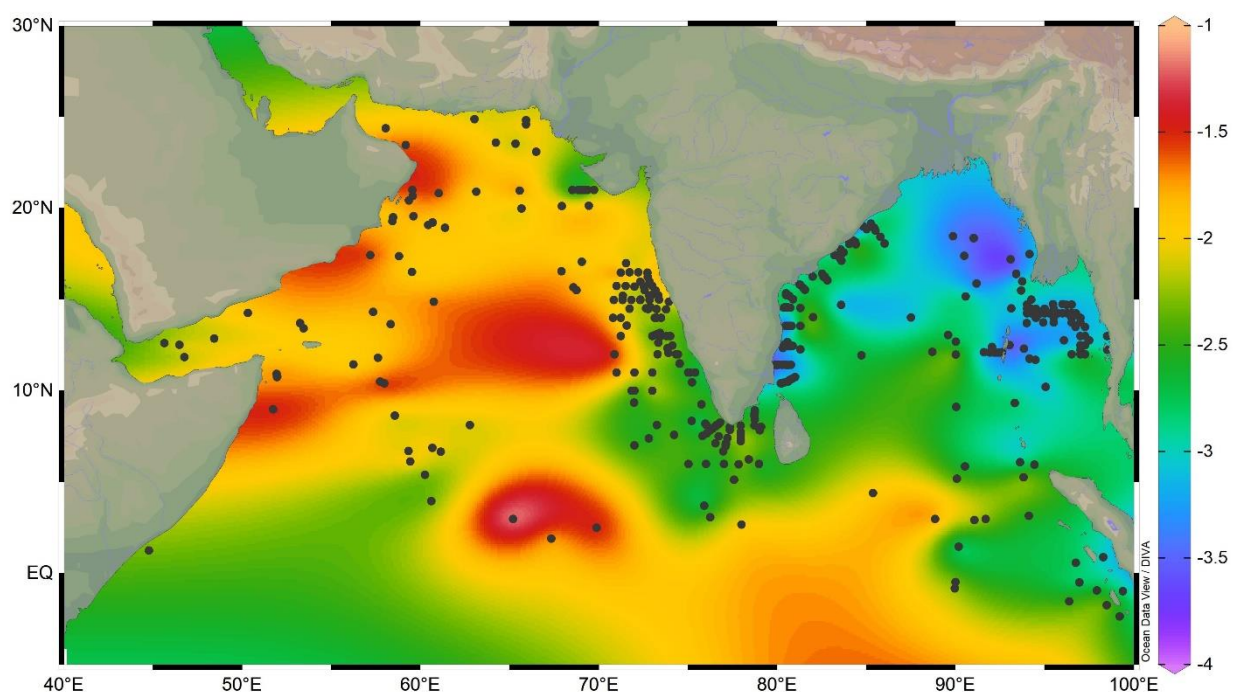
184 The analyzed $\delta^{18}\text{O}_{ruber}$ data was compared with the expected $\delta^{18}\text{O}$ calcite to ascertain whether the *G. ruber*
 185 properly represents the ambient conditions. For the expected $\delta^{18}\text{O}$ calcite, the $\delta^{18}\text{O}_{sw}$ was calculated from the ambient
 186 salinity by using a compilation of the regional seawater salinity and its stable oxygen isotopic ($\delta^{18}\text{O}_{sw}$) ratio data for

187 the entire northern Indian Ocean (5°S to 30°N). The seawater salinity and corresponding $\delta^{18}\text{O}_{\text{sw}}$ data was downloaded
188 from the Schmidt et al., (1999) (version 1.22) and augmented with other regional datasets (Delaygue et al., 2001;
189 Singh et al., 2010; Achyuthan et al., 2013).

190

191 5. Results

192 The oxygen isotopic ratio of *G. ruber* varies from a minimum of -3.82‰ to the maximum of -1.09‰ in the surface
193 sediments of the northern Indian Ocean (Figure 3). The most depleted $\delta^{18}\text{O}_{\text{ruber}}$ was in the eastern BoB and the most
194 enriched values were in the western Arabian Sea.

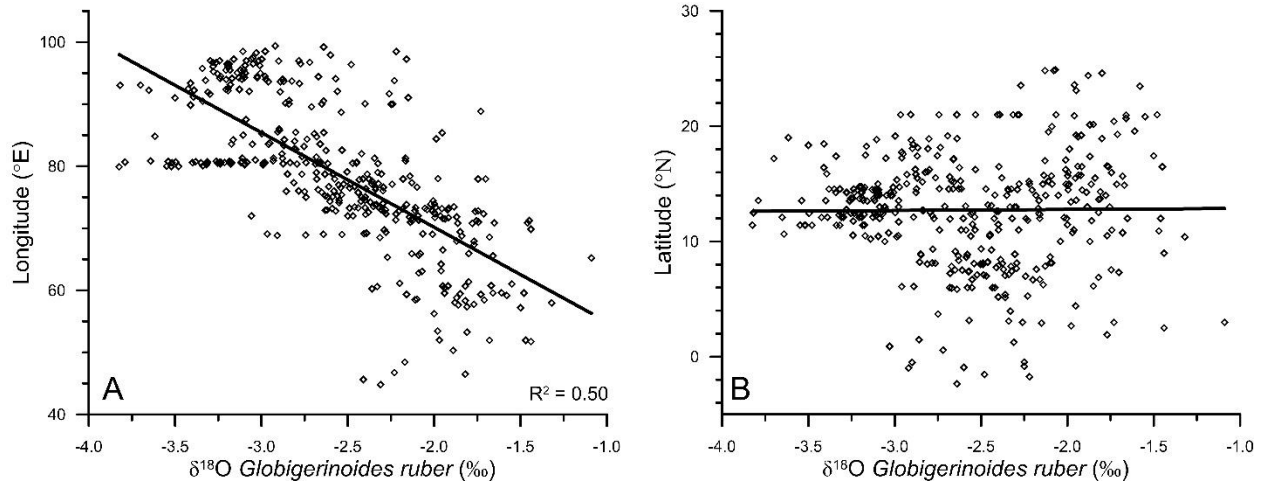


195
196

197 **Figure 3: The variation in *Globigerinoides ruber* $\delta^{18}\text{O}$ (‰) in the surface sediments of the northern Indian Ocean. The**
198 **stations are marked by black filled circle. The lowest $\delta^{18}\text{O}_{\text{ruber}}$ is in the riverine influx influenced northern Bay of Bengal**
199 **and the highest is in the evaporation dominated central and western Arabian Sea. The major rivers are marked with thin**
200 **blue lines. The map was prepared by using Ocean Data View software (Schlitzer, 2018).**

201

202 The east-west gradient in $\delta^{18}\text{O}_{\text{ruber}}$ was also evident in its significant correlation ($R^2 = 0.5$, $n = 400$) with the longitude
203 (Figure 4A). However, $\delta^{18}\text{O}_{\text{ruber}}$ did not have any systematic latitudinal variation (Figure 4B).

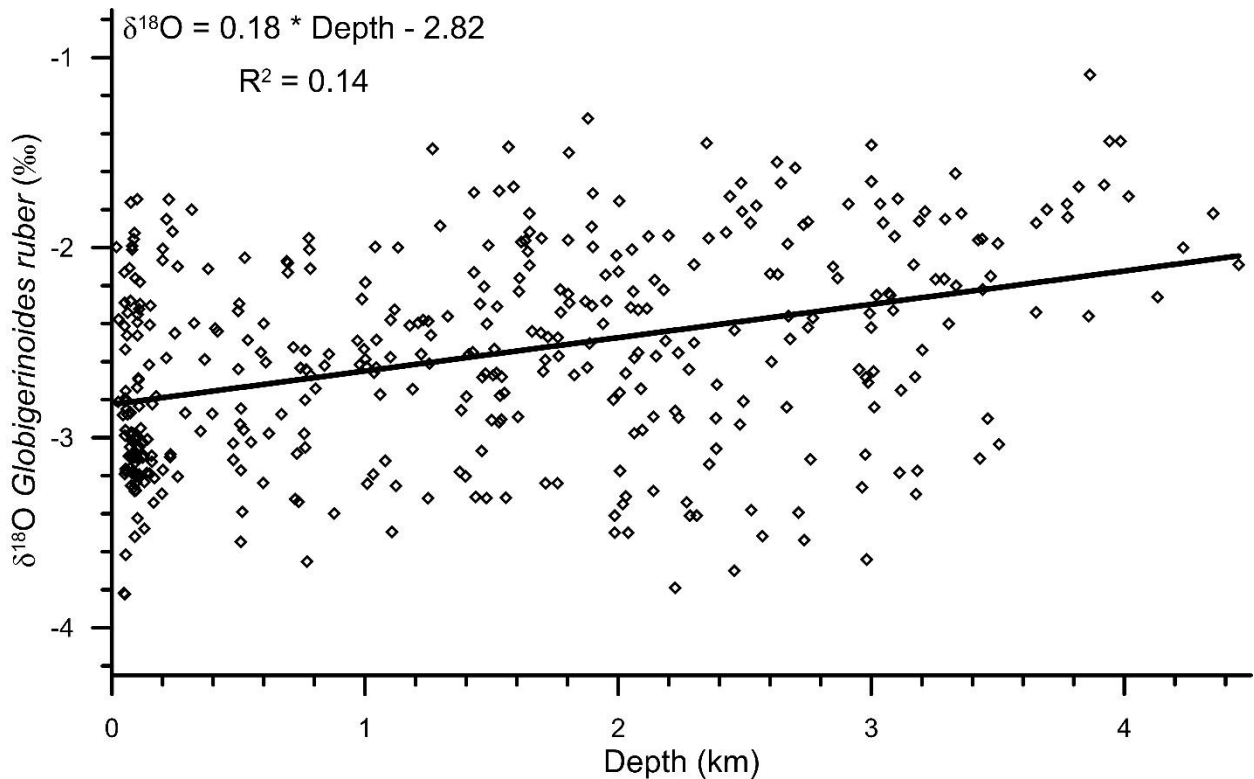


204
205
206
207
208

Figure 4: The variation in *Globigerinoides ruber* $\delta^{18}\text{O}$ (‰) with the corresponding longitude (A) and latitude (B), in the surface sediments of the northern Indian Ocean. The correlation between $\delta^{18}\text{O}_{ruber}$ and latitude of the sample, is insignificant.

209

210 A significant correlation ($R^2 = 0.14$, $n = 400$) was observed between the water depth and $\delta^{18}\text{O}_{ruber}$ (Figure 5). $\delta^{18}\text{O}_{ruber}$
211 increased with increasing depth. The increase was gradual, without any abrupt change.

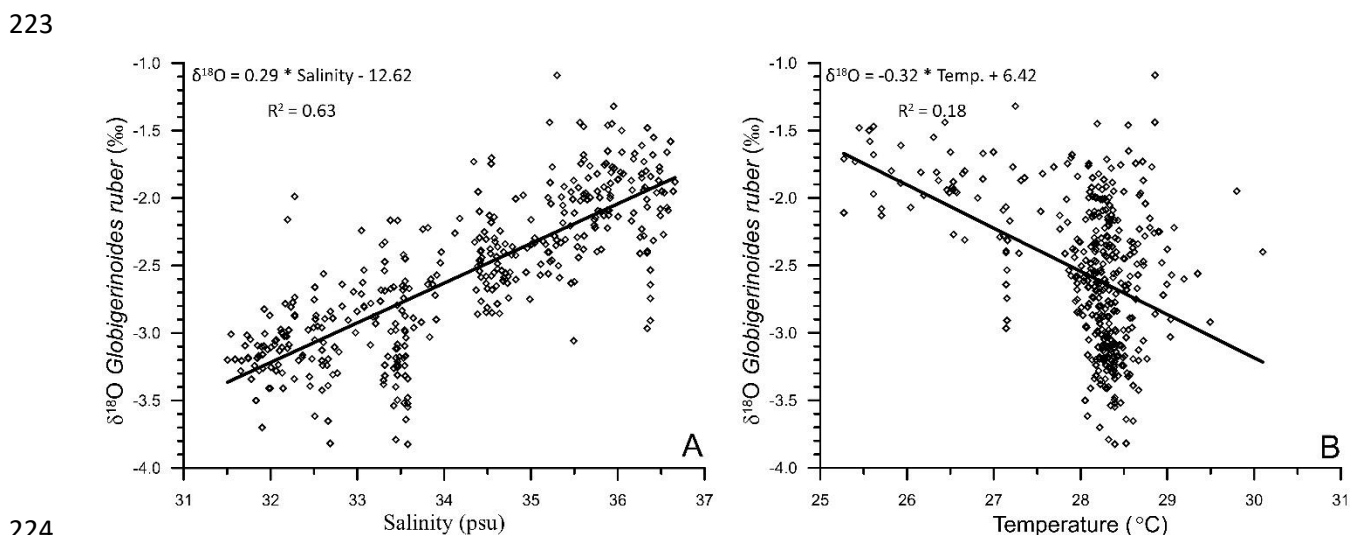


212
213
214
215

Figure 5: The relationship between water depth and the oxygen isotopic ratio of the mixed layer dwelling *Globigerinoides ruber* in the surface sediments of the northern Indian Ocean. The trendline signifies the relative enrichment of $\delta^{18}\text{O}_{ruber}$

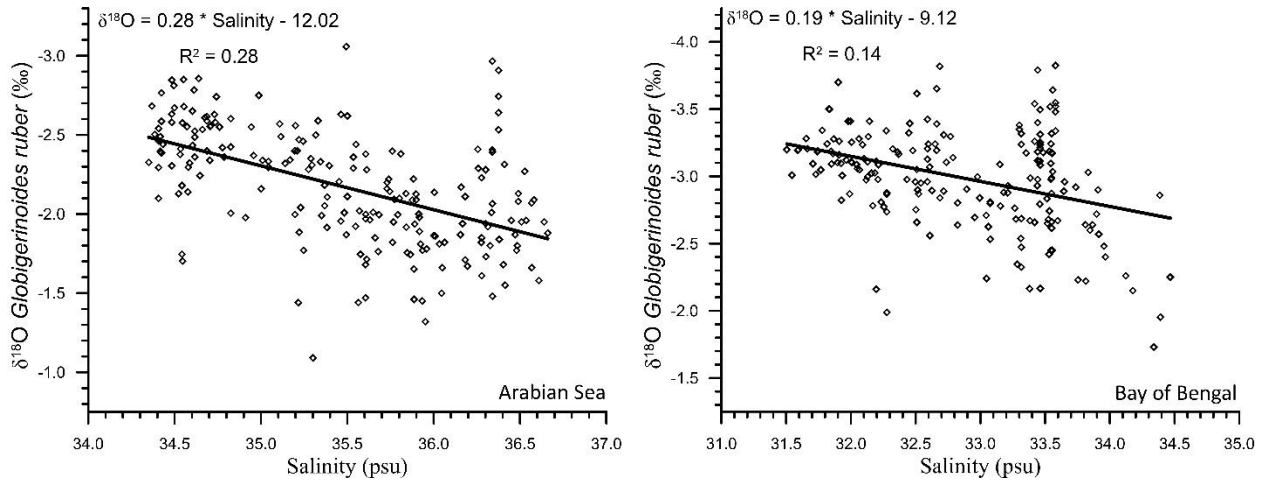
216 shells in surface sediments, with increasing water depth. The empirical relationship between the water depth and $\delta^{18}\text{O}_{ruber}$
217 is represented with an equation. The $\delta^{18}\text{O}_{ruber}$ is significantly correlated ($R^2 = 0.14$, $n = 400$) with the water depth.

218
219 The uncorrected $\delta^{18}\text{O}_{ruber}$ was significantly correlated ($R^2 = 0.63$, $n = 400$) with the ambient salinity (Figure 6A).
220 However, the relationship between uncorrected $\delta^{18}\text{O}_{ruber}$ and ambient temperature was not as robust ($R^2 = 0.18$, $n =$
221 400) (Figure 6B). A large scatter ($\sim -3.8\text{‰}$ to -1.4‰) was observed in the $\delta^{18}\text{O}_{ruber}$ of the samples collected from a
222 narrow range of ambient temperature (28-29°C) (Figure 6B).



225
226 **Figure 6: The relationship between the stable oxygen isotopic ratio of the mixed layer dwelling *Globigerinoides ruber* and**
227 **annual average mixed layer salinity (A), and temperature (B) in the northern Indian Ocean.**

228
229 As the northern Indian Ocean includes two contrasting basins, $\delta^{18}\text{O}_{ruber}$ -salinity relationship was explored for both the
230 Arabian Sea and the BoB. A significant $\delta^{18}\text{O}_{ruber}$ -salinity relationship was observed for both the Arabian Sea ($R^2 =$
231 0.28, $n = 205$) and BoB ($R^2 = 0.14$, $n = 195$) (Figure 7). We report a different $\delta^{18}\text{O}_{ruber}$ -salinity relationship in these
232 two basins. $\delta^{18}\text{O}_{ruber}$ increased with increasing salinity in both the BoB and the Arabian Sea.



233

234

235

236

237

Figure 7: The relationship between the stable oxygen isotopic ratio of mixed layer dwelling *Globigerinoides ruber* and annual average mixed layer salinity in the Arabian Sea and Bay of Bengal.

238

239

240

241

242

243

244

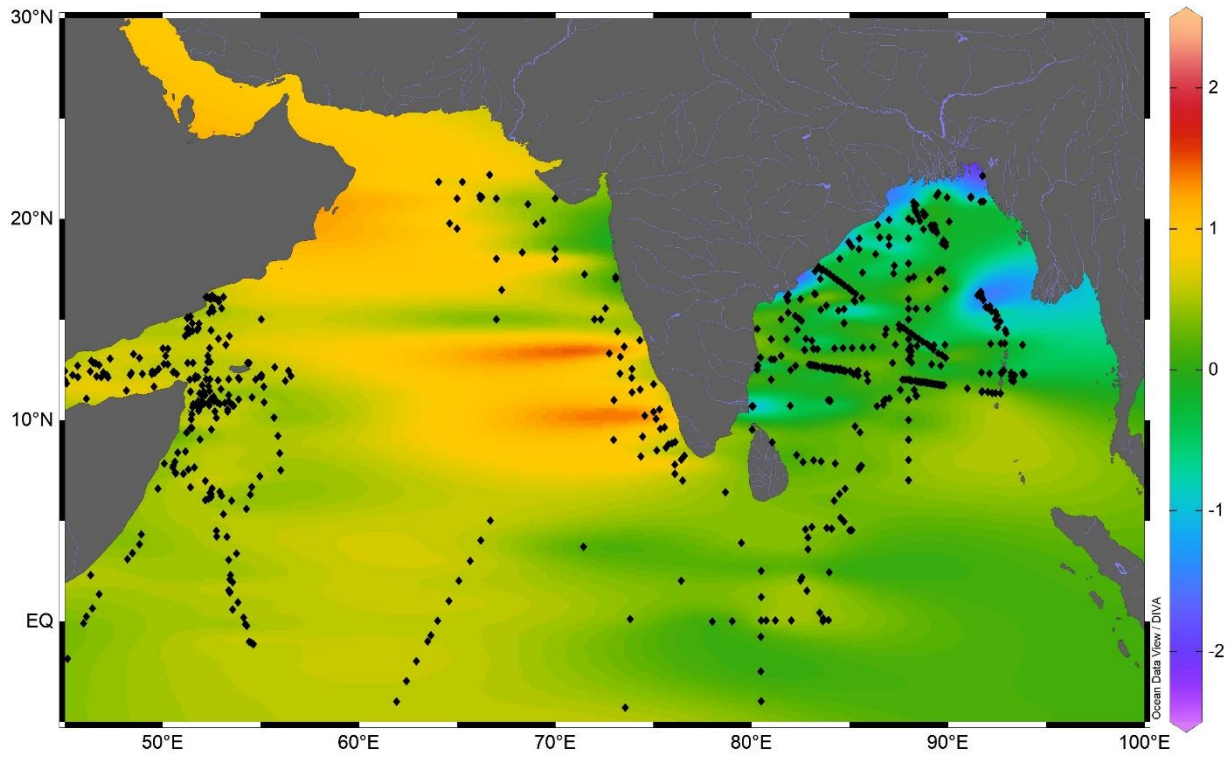
245

246

247

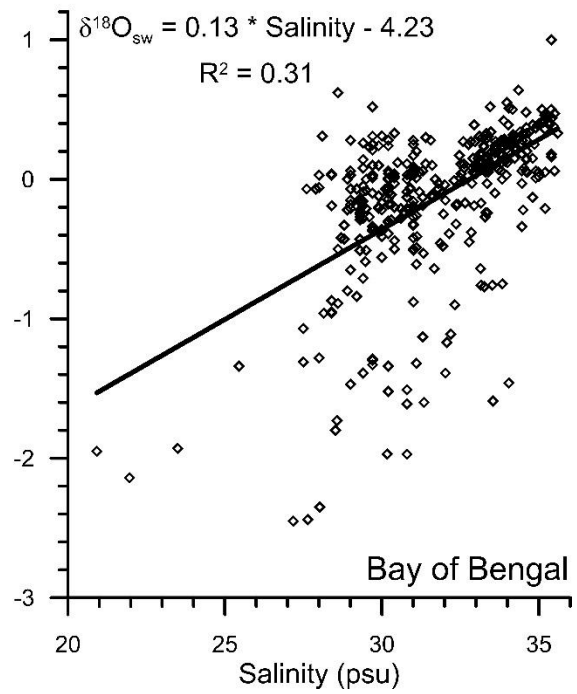
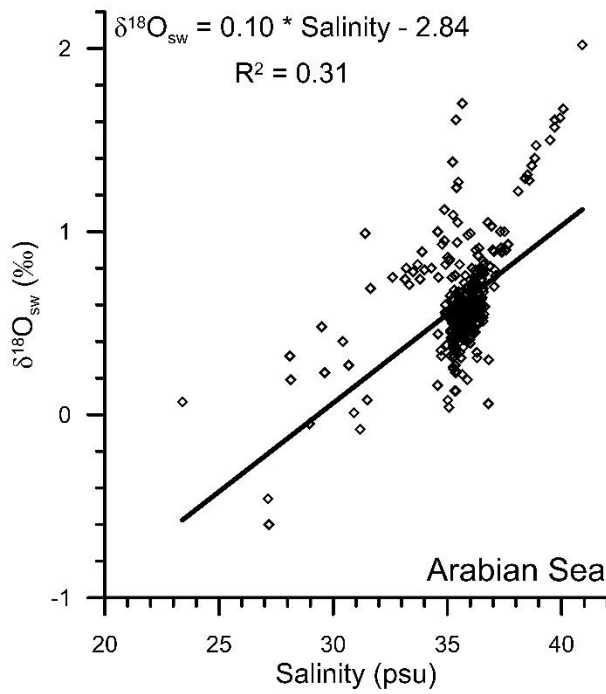
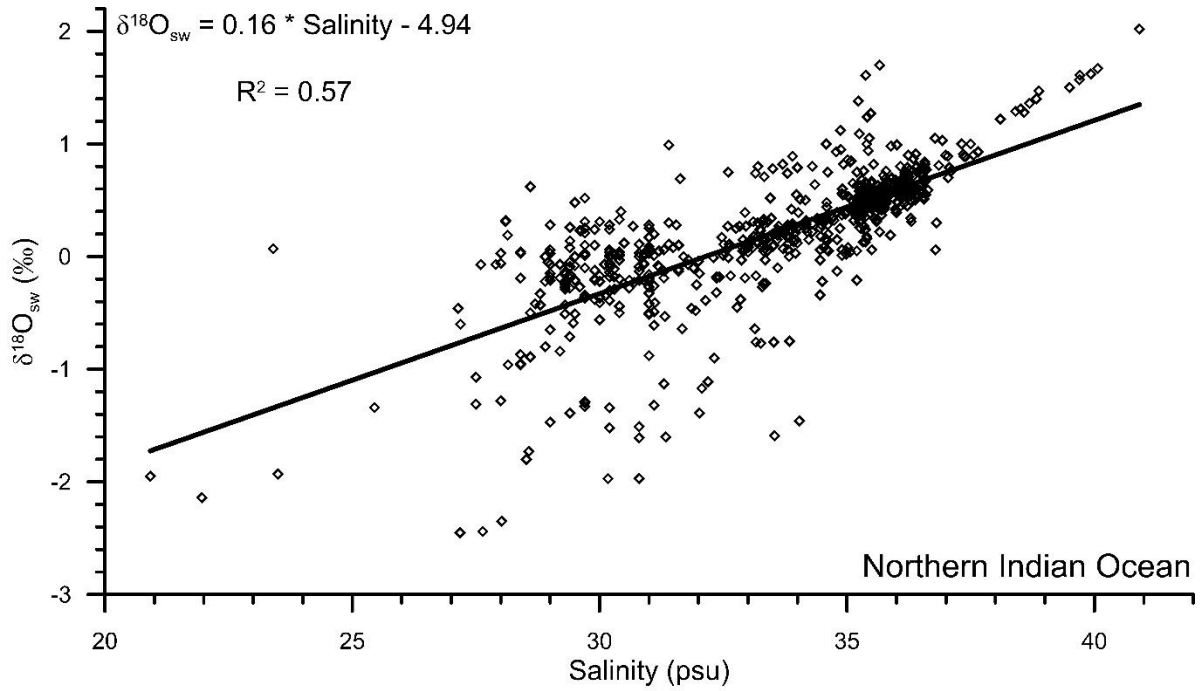
248

The dataset to derive the regional salinity- $\delta^{18}\text{O}_{\text{sw}}$ relationship comprised of a total of 750 stations with salinity varying from 20.92 psu to 40.91 psu. The dataset also covered a large range of $\delta^{18}\text{O}_{\text{sw}}$, varying from a minimum of -2.45‰ to the maximum of 2.02‰ (Figure 8, 9). The measured $\delta^{18}\text{O}_{\text{ruber}}$ was strongly correlated ($R^2 = 0.56$, $n = 400$) with the expected $\delta^{18}\text{O}_{\text{calcite}}$, as estimated by using the salinity- $\delta^{18}\text{O}_{\text{sw}}$ relationship and the ambient temperature. However, the relationship between seawater temperature and $\delta^{18}\text{O}_{\text{ruber}} - \delta^{18}\text{O}_{\text{sw}}$, was not very robust. It should however, be noted here that the stratigraphic information is not provided for most of the core tops. The core top sediments can represent older time slices when the sedimentation rates are low or when older sediments are exposed due to erosional processes. This does not matter so much if the Holocene is present and stable. However, in the Indian Ocean, large Holocene $\delta^{18}\text{O}$ variations are expected due to variations in monsoon precipitation. Therefore, the uncertain age of the core tops can affect the results stated above.



249
 250
 251
 252
 253
 254

Figure 8: The surface seawater oxygen isotopic ratio (‰) in the northern Indian Ocean. The black filled circles are the seawater sample locations compiled from previous studies. The thin blue lines are the major rivers draining in the northern Indian Ocean. The map was prepared by using Ocean Data View software (Schlitzer, 2018).



255
256
257

258 **Figure 9:** The relationship between surface water oxygen isotopic ratio and salinity in the northern Indian Ocean (5°S-
259 30°N), Arabian Sea and the Bay of Bengal. The data points are from Schmidt et al., (1999), Delaygue et al., (2001), Singh et
260 al., (2010), and Achyuthan et al., (2013).

261

262 6. Discussion

263 6.1 Expected versus analyzed $\delta^{18}\text{O}$

264 The seawater $\delta^{18}\text{O}$ data is required to estimate the expected $\delta^{18}\text{O}$ carbonate. The seawater $\delta^{18}\text{O}$, however, was not
265 measured. Therefore, the salinity- $\delta^{18}\text{O}_{\text{sw}}$ relationship established from the previous regional seawater isotope and
266 salinity measurements was used. The salinity- $\delta^{18}\text{O}_{\text{sw}}$ relationship varies seasonally as well as from region to region
267 (Singh et al., 2010; Achyuthan et al., 2013; Tiwari et al., 2013). Therefore, it was difficult to choose the appropriate
268 salinity- $\delta^{18}\text{O}_{\text{sw}}$ relationship. Initially, all the data points were clubbed to establish the salinity- $\delta^{18}\text{O}_{\text{sw}}$ relationship. By
269 comparing the measured $\delta^{18}\text{O}_{\text{sw}}$ with the ambient salinity, we established the following relationship for the entire
270 northern Indian Ocean (north of 5°S latitude) ($R^2 = 0.57$, $n = 750$) (Figure 9).

271

$$272 \delta^{18}\text{O}_{\text{sw}} = 0.16 * \text{Salinity} - 4.94 \quad \text{Northern Indian Ocean } (R^2 = 0.57)$$

273

274 Previously, a large difference in the slope of salinity- $\delta^{18}\text{O}_{\text{sw}}$ equation has been reported from the Arabian Sea and the
275 BoB (Delaygue et al., 2001; Singh et al., 2010; Achyuthan et al., 2013). Therefore, we also plotted the salinity- $\delta^{18}\text{O}_{\text{sw}}$
276 separately for the Arabian Sea and BoB (Figure 9). The salinity- $\delta^{18}\text{O}_{\text{sw}}$ relationship for these two basins was
277 represented by the following equations.

278

$$279 \delta^{18}\text{O}_{\text{sw}} = 0.10 * \text{Salinity} - 2.84 \quad \text{Arabian Sea} \quad (R^2 = 0.31, n = 375)$$

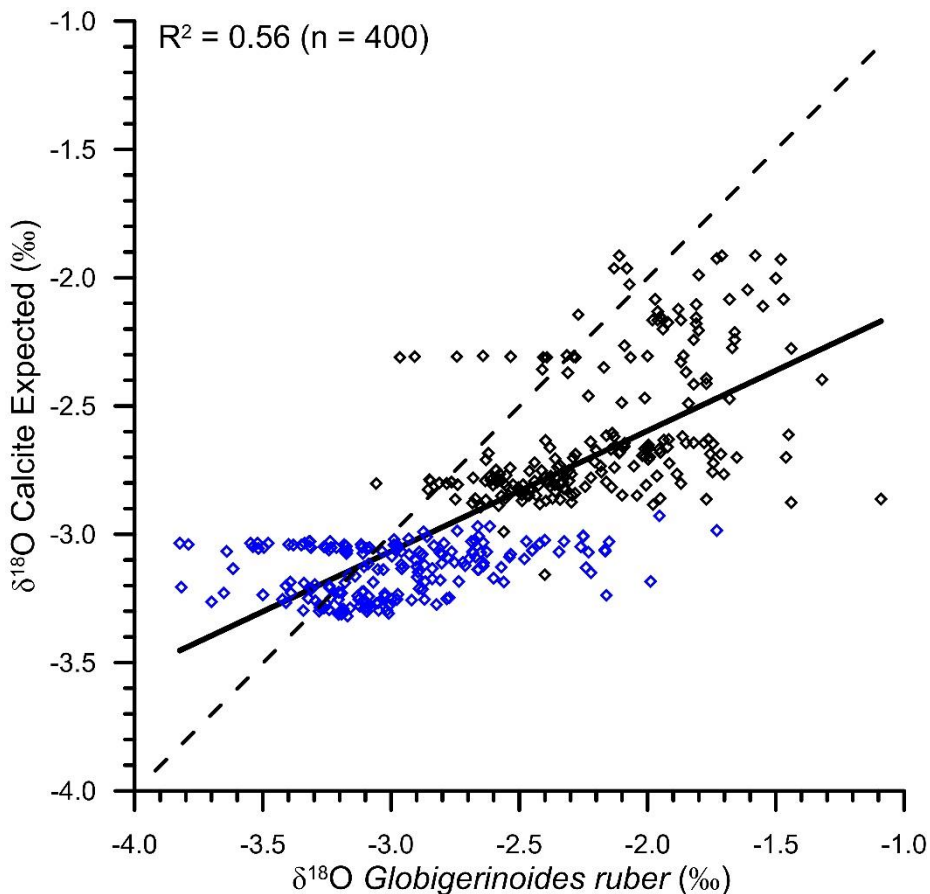
280

$$281 \delta^{18}\text{O}_{\text{sw}} = 0.13 * \text{Salinity} - 4.23 \quad \text{Bay of Bengal} \quad (R^2 = 0.31, n = 375)$$

282

283 The continuous flux of *G. ruber* throughout the year (Guptha et al., 1997) and the accumulation of shells in the
284 sediments over a large interval, implies that the salinity- $\delta^{18}\text{O}_{\text{sw}}$ relationship based on data representing all seasons will
285 provide a better estimate of the average $\delta^{18}\text{O}_{\text{ruber}}$ as recovered from the sediments (Vergnaud-Grazzini, 1976). The
286 expected $\delta^{18}\text{O}_{\text{sw}}$ was calculated by using these equations and the annual average mixed layer salinity at the stations
287 for which $\delta^{18}\text{O}_{\text{ruber}}$ data were available. The mixed layer was defined as the top 25 m of the water column following
288 Narvekar and Prasanna Kumar (2014). Although the mixed layer depth varies regionally as well as during different
289 seasons, the average mixed layer depth was used to compare the calcification conditions. A correction factor of 0.27‰
290 was applied to convert $\delta^{18}\text{O}_{\text{sw}}$ from Standard Mean Oceanic Water scale (SMOW) to Pee Dee Belemnite scale (PDB)
291 (Hut, 1987). The expected $\delta^{18}\text{O}$ calcite was then estimated from the calculated $\delta^{18}\text{O}_{\text{sw}}$ and the annual average mixed
292 layer temperature by using the equation proposed by Mulitza et al., (2003). We also estimated the expected $\delta^{18}\text{O}$
293 calcite by using the high-light equation of Bemis et al (1998), as *G. ruber* $\delta^{18}\text{O}$ is better described with the high-light
294 equation (Thunell et al., 1999). The choice of equation used to estimate the expected $\delta^{18}\text{O}$ calcite did not make any
295 difference other than a small offset. The difference between expected $\delta^{18}\text{O}$ calcite estimated by using paleotemperature
296 equation of Mulitza et al., (2003) and the high-light equation of Bemis et al., (1998) varied from -0.33 to -0.41‰. The
297 expected $\delta^{18}\text{O}$ calcite estimated by using Mulitza et al., (2003) paleotemperature equation provided values close to the

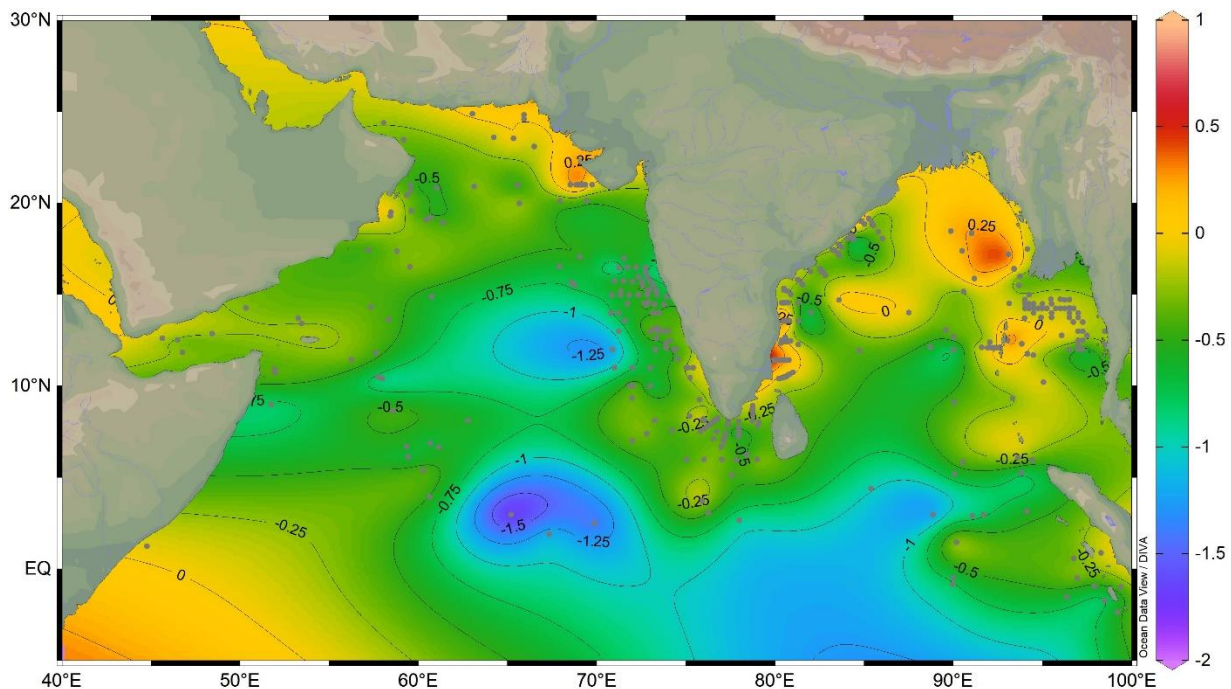
298 measured *G. ruber* $\delta^{18}\text{O}$. From the scatter plot (Figure 10), it was clear that the analyzed $\delta^{18}\text{O}_{ruber}$ was significantly
 299 correlated ($R^2 = 0.56$, $n = 400$) with the expected $\delta^{18}\text{O}$ calcite, suggesting that *G. ruber* closely represents the ambient
 300 conditions in the entire northern Indian Ocean. The expected $\delta^{18}\text{O}$ calcite estimated by using the separate Arabian Sea
 301 and BoB salinity- $\delta^{18}\text{O}_{sw}$ equations, was also similarly correlated with the analyzed $\delta^{18}\text{O}_{ruber}$.



302
 303
 304 **Figure 10: The scatter plot of expected $\delta^{18}\text{O}$ calcite (as estimated from the ambient salinity-temperature) and the analyzed**
 305 **$\delta^{18}\text{O}_{ruber}$. The two are significantly correlated ($R^2 = 0.56$), suggesting that *Globigerinoides ruber* correctly represents the**
 306 **ambient conditions. The blue diamonds are the samples collected from the Bay of Bengal and the black diamonds represent**
 307 **the samples collected from the Arabian Sea. The dotted line represents the 1:1 relationship between the measured and**
 308 **expected $\delta^{18}\text{O}$.**

309
 310 The deviation of the expected $\delta^{18}\text{O}_{calcite}$ from the observed $\delta^{18}\text{O}_{ruber}$ ($\delta^{18}\text{O}_{residual}$) can be because of several factors
 311 including the difference in the ambient conditions at the time of secretion of the primary calcite during the lifetime
 312 and the diagenetic changes post death and burial. The observed $\delta^{18}\text{O}_{ruber}$ was close to the expected $\delta^{18}\text{O}_{calcite}$ in the
 313 shallower waters, especially the BoB, Andaman Sea and northeastern Arabian Sea (Figure 11). The difference was
 314 large in the deeper Arabian Sea and the equatorial Indian Ocean. *Globigerinoides ruber* is suggested to inhabit
 315 chlorophyll maximum for easy availability of food (Fairbanks and Weibe, 1980). In such a scenario, $\delta^{18}\text{O}_{ruber}$ is
 316 expected to be higher due to lower temperatures and lower light levels at relatively deeper depths (Spero et al., 1997).
 317 The depth of chlorophyll maximum is shallower in the marginal marine waters of both the BoB and the Arabian Sea

318 (Sarma & Aswanikumar, 1991; Madhu et al., 2006). If *G. ruber* thrived at chlorophyll maximum depths, the $\delta^{18}\text{O}_{ruber}$
 319 should be enriched in heavier isotope and thus $\delta^{18}\text{O}_{residual}$ should be negative. The positive $\delta^{18}\text{O}_{residual}$ in the shallower
 320 regions, however, suggests that *G. ruber* thrives in the warmer upper parts of the mixed layer. Alternatively, the large
 321 influence of the depleted fresh water $\delta^{18}\text{O}$ dominates the chlorophyll maximum influence on the observed $\delta^{18}\text{O}_{ruber}$ in
 322 the shallower regions of the northern Indian Ocean. The concentration of positive $\delta^{18}\text{O}_{residual}$ values close to the riverine
 323 influx regions confirms the strong influence of the depleted fresh water $\delta^{18}\text{O}$ in modulating $\delta^{18}\text{O}_{ruber}$ in the northern
 324 Indian Ocean. The negative $\delta^{18}\text{O}_{residual}$ at deeper stations is attributed to a combination of factors including deeper
 325 chlorophyll maximum depth habitat of *G. ruber*, reduced influence of fresh water, lower sedimentation rate resulting
 326 in mixing of older and younger fauna, and post depositional diagenetic changes.



327
 328 **Figure 11: The difference in the expected $\delta^{18}\text{O}_{calcite}$ and observed $\delta^{18}\text{O}_{ruber}$ ($\delta^{18}\text{O}_{residual}$) in the surface sediments of the**
 329 **northern Indian Ocean. The grey filled squares are the sample locations. The thin blue lines are the major rivers draining**
 330 **in the northern Indian Ocean. The thin black lines mark the contours at 0.25‰ interval. The map was prepared by using**
 331 **Ocean Data View software (Schlitzer, 2018).**

332

333 6.2 Latitudinal and Longitudinal variation in $\delta^{18}\text{O}_{ruber}$

334 We report a strong ($R^2 = 0.50$) longitudinal influence on $\delta^{18}\text{O}_{ruber}$. A similar relationship with the latitudes is missing.
 335 The strong longitudinal signature in $\delta^{18}\text{O}_{ruber}$ is attributed to the large salinity gradient. The huge fresh water influx in
 336 the BoB reduces the SSS in the eastern Indian Ocean. The lack of major rivers in the western Arabian Sea results in
 337 strong low to high salinity gradient from east to west. Although the equatorial and nearby regions are a part of the

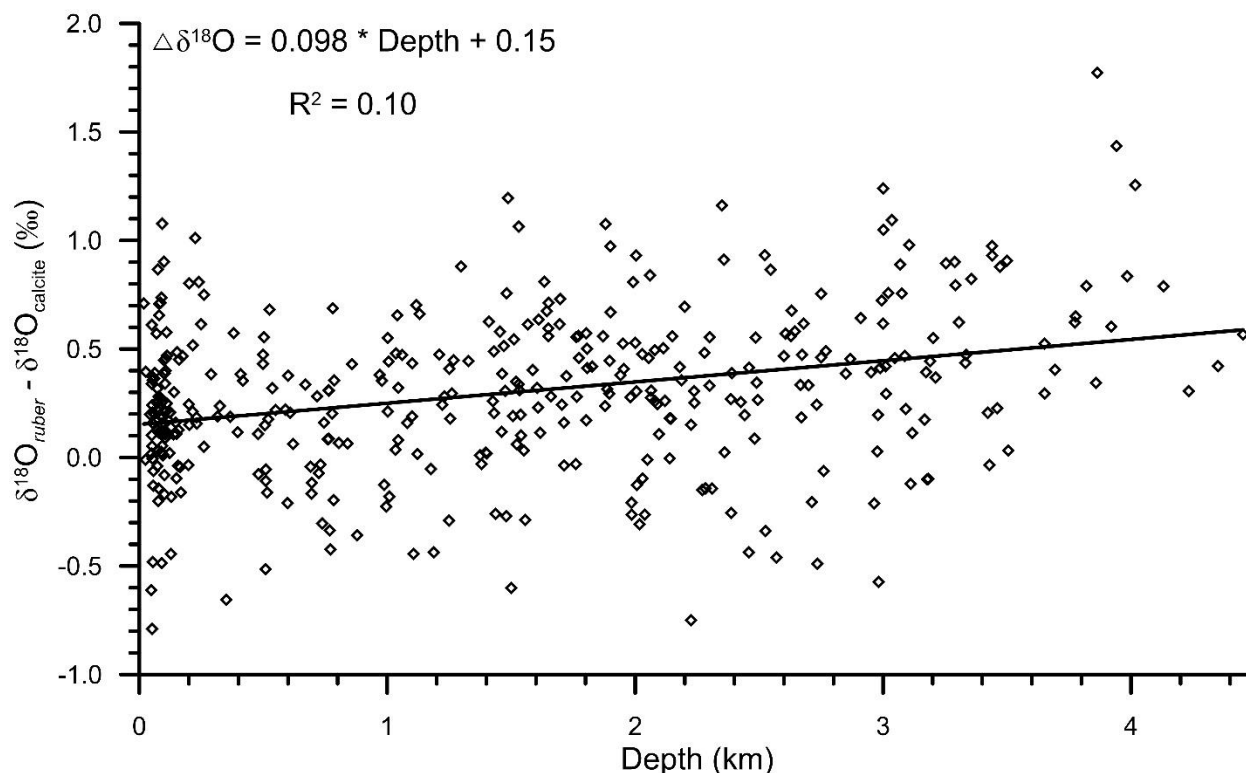
338 Indo-Pacific Warm Pool, the limited temperature variability is evident in the insignificant latitudinal influence on
339 $\delta^{18}\text{O}_{ruber}$.
340

341 **6.3 Diagenetic alteration**

342 We found a strong diagenetic overprinting of $\delta^{18}\text{O}_{ruber}$ in the northern Indian Ocean (Figure 5). The enrichment of
343 $\delta^{18}\text{O}_{ruber}$ with increasing water depth suggests either dissolution leading to the preferential removal of chambers with
344 higher fraction of the lighter oxygen isotope (Wycech et al., 2018), or secondary calcification under comparatively
345 colder water (Lohmann, 1995; Schrag et al., 1995). The increase in planktic foraminifera $\delta^{18}\text{O}$ with increasing depth
346 is a common diagenetic alteration throughout the world oceans (Bonneau et al., 1980). Interestingly, the extent of the
347 increase in $\delta^{18}\text{O}_{ruber}$ with depth in the northern Indian Ocean is much smaller (0.18‰ per thousand meters) than that
348 reported for the same species from the Pacific Ocean (0.4‰ per thousand meters) (Bonneau et al., 1980). However,
349 the increase in $\delta^{18}\text{O}_{ruber}$ with depth in the northern Indian Ocean is continuous, unlike the abrupt shift in $\delta^{18}\text{O}$ (0.3-
350 0.4‰, between the depths above and below the lysocline) of another surface dwelling planktic species, namely
351 *Trilobatus sacculifer*, as observed in the western equatorial Pacific (Wu and Berger, 1989). The smaller increase in
352 $\delta^{18}\text{O}_{ruber}$ with depth is attributed to the shallower habitat of *G. ruber* as compared to *T. sacculifer*. The chamber
353 formation at different water depths implies increased heterogeneity in the *T. sacculifer* shells, with those formed at
354 warmer surface temperature being more susceptible to dissolution as compared to those formed at deeper depths during
355 the gametogenesis phase (Wycech et al., 2018). The chambers in *G. ruber* are formed at a similar depth and therefore,
356 the increase in $\delta^{18}\text{O}_{ruber}$ is continuous, while those of *T. sacculifer* are precipitated at different depths and therefore the
357 shift in $\delta^{18}\text{O}$ after a particular depth. The increase in $\delta^{18}\text{O}_{ruber}$ with depth is mainly due to the partial dissolution of the
358 more porous and thinner parts of the shells secreted at warmer temperature, as such parts are comparatively more
359 susceptible to dissolution (Berger, 1971). The increase in $\delta^{18}\text{O}_{ruber}$ with depth is similar in both the Arabian Sea and
360 BoB.

361 Additionally, the gradual decrease in the sedimentation rate with increasing depth and distance from the
362 continental margins can also induce a depth related trend in $\delta^{18}\text{O}_{ruber}$. The bioturbation disturbs the top few cm of the
363 sediments (Gerino et al., 1998), mixing older shells with comparatively younger shells (Löwemark, and Grootes,
364 2004). In high sedimentation rate regions of the shelf and slope, the mixing is restricted to the shells deposited in a
365 shorter, climatologically stable interval. However, in the deeper regions, it is likely that the shells deposited during
366 the colder glacial interval or deglaciation with relatively higher $\delta^{18}\text{O}_{ruber}$ gets mixed with the younger shells, as it is
367 available close to the surface due to the low sedimentation rate (Broecker, 1986; Anderson, 2001). The mixing of
368 shells with a relatively higher $\delta^{18}\text{O}$ with the modern shells having lighter $\delta^{18}\text{O}$ can also result in the depth related
369 increasing trend of $\delta^{18}\text{O}_{ruber}$. The sedimentation rate is very high on the slope and decreases in the deeper regions of
370 both the Arabian Sea (Singh et al., 2017) and BoB (e.g. Bhonsale and Saraswat, 2012; Suokhrie et al., 2022). However,
371 it should be noted here that the sedimentation rate in large parts of the BoB is still high enough to prevent availability
372 of deglacial or last glacial maximum shells within the bioturbation induced mixing limits.

373 The large influence of the terrestrial fresh water influx in the shallower region, as compared to the deeper
 374 parts of the northern Indian Ocean, is also likely to contribute to the observed increase in $\delta^{18}\text{O}_{ruber}$ with depth. The
 375 fresh water is depleted in heavier oxygen isotope as compared to the seawater (Bhattacharya et al., 1985; Ramesh &
 376 Sarin, 1992). Thus, the foraminiferal shells secreted in the shallow waters are likely to be enriched in the lighter
 377 oxygen isotope, resulting in a depth related bias. Therefore, to delineate the influence of depth related diagenetic
 378 alteration and secondary calcification in $\delta^{18}\text{O}_{ruber}$, we subtracted the expected $\delta^{18}\text{O}_{calcite}$ from the measured $\delta^{18}\text{O}_{ruber}$.
 379 The difference between the measured $\delta^{18}\text{O}_{ruber}$ and expected $\delta^{18}\text{O}_{calcite}$ was plotted with water depth (Figure 12). The
 380 difference (measured $\delta^{18}\text{O}_{ruber}$ - expected $\delta^{18}\text{O}_{calcite}$) increased with depth, suggesting a strong influence of the depth
 381 related processes in $\delta^{18}\text{O}_{ruber}$.



382
 383 **Figure 12: The relationship of the difference between measured $\delta^{18}\text{O}_{ruber}$ and expected $\delta^{18}\text{O}_{calcite}$ with the water depth from**
 384 **which the surface samples were collected, in the northern Indian Ocean. The $\delta^{18}\text{O}_{ruber} - \delta^{18}\text{O}_{calcite}$ increased with increasing**
 385 **water depth.**

386

387 6.4 Salinity contribution to $\delta^{18}\text{O}_{ruber}$

388 We report a strong influence of the fresh water influx induced salinity on $\delta^{18}\text{O}_{ruber}$ ($R^2=0.63$). As expected, $\delta^{18}\text{O}_{ruber}$
 389 has a direct positive relationship with the ambient salinity. The $\delta^{18}\text{O}_{ruber}$ increased by 0.29‰ for every psu increase in
 390 salinity. The northern Indian Ocean has a large salinity gradient (~10 psu) from the lowest in the northern BoB to the
 391 highest in the northwestern Arabian Sea, mainly driven by the fresh water input. The river water and direct
 392 precipitation is enriched in the lighter isotope (Kumar et al., 2010; Kathayat et al., 2021). Thus, the increased riverine

393 influx and precipitation contributes isotopically lighter water to the surface ocean (Rai et al., 2021) and decreases the
394 $\delta^{18}\text{O}_{ruber}$. From the surface seawater samples collected during the winter monsoon season (January-February 1994), a
395 $\delta^{18}\text{O}$ -salinity slope of 0.26‰ was deduced for the Arabian Sea and of 0.18‰ for the BoB (Delaygue et al., 2001).
396 However, the $\delta^{18}\text{O}$ -salinity slope varies regionally as well as during different seasons (Singh et al., 2010; Achyuthan
397 et al., 2013). The $\delta^{18}\text{O}$ -salinity slope varied from as low as 0.10 for the coastal BoB samples collected during the
398 months of April-May to as high as 0.51 for the samples collected from the western BoB during the peak south-west
399 monsoon season (August-September 1988) (Singh et al., 2010). The large seasonal variation implies limitations of
400 $\delta^{18}\text{O}$ -salinity slope deduced from snapshot surface seawater samples. Additionally, *G. ruber* flux is reported
401 throughout the year (Guptha et al., 1997), suggesting that the fossil population represents annual average conditions
402 (Thirumalai et al., 2014).

403 A different $\delta^{18}\text{O}_{ruber}$ -salinity slope for the Arabian Sea (0.28) and BoB (0.19) is attributed to the different
404 hydrographic regimes of these two basins. The runoff and precipitation excess in the BoB results in a comparatively
405 lower salinity as compared to the evaporation dominated Arabian Sea. However, it should be noted here that the
406 relationship between $\delta^{18}\text{O}_{ruber}$ and salinity was very robust for all the northern Indian Ocean samples plotted together.
407 Interestingly, the slope of $\delta^{18}\text{O}$ -salinity for the entire northern Indian Ocean samples is much lower than that for the
408 Atlantic Ocean (0.59 for North Atlantic and 0.52 for South Atlantic, Delaygue et al., 2000) despite the large meltwater
409 influx into the north Atlantic. The dissimilar $\delta^{18}\text{O}$ -salinity slope in different basins and also during different seasons
410 in the same basin is mainly attributed to the variation in the end member composition and the relative amount of fresh
411 water (riverine/precipitation/sub-marine ground water discharge) input from various sources during different seasons
412 (Achyuthan et al., 2013; Tiwari et al., 2013). The heavier oxygen isotope depleted precipitation/fresh water influx in
413 the higher latitudes (~-35 ‰) as compared to the tropical areas (~-5 ‰) also results in a higher slope of the $\delta^{18}\text{O}$ -
414 salinity relationship in the North Atlantic Ocean (Rozanski et al., 1993). Additionally, the difference in $\delta^{18}\text{O}$ -salinity
415 slope despite of the huge fresh water input into both the basins is also because a large fraction of the riverine fresh
416 water spreads across the surface of the northern Indian Ocean, while the melt water sinks to deeper depths in the North
417 Atlantic Ocean. A consistent systematic difference has previously been observed between planktic foraminiferal shells
418 collected in plankton tows and surface sediments, with shells from the sediments being comparatively enriched in ^{18}O
419 (Vergnaud-Grazzini, 1976).

420

421 **6.5 Temperature control on $\delta^{18}\text{O}_{ruber}$**

422 A first order comparison of the uncorrected $\delta^{18}\text{O}_{ruber}$ with ambient temperature of the top 30 m of the water column at
423 respective stations showed 0.32‰ decrease with every 1°C warming. The change in $\delta^{18}\text{O}_{ruber}$ as inferred from the
424 core-top sediments of the northern Indian Ocean is higher than that estimated from the plankton tows (0.22‰ per 1°C
425 change in temperature) (Mullitza et al., 2003). The seawater temperature was amongst the primary factors identified
426 to affect $\delta^{18}\text{O}_{ruber}$ (Emiliani, 1954; Mullitza et al., 2003). The low correlation between $\delta^{18}\text{O}_{ruber}$ and temperature in this
427 dataset is attributed to the limited temperature variability (1°C, 28-29°C) at a majority of the stations. The large salinity

428 difference (~6.5 psu) between stations further obscures any significant correlation between uncorrected $\delta^{18}\text{O}_{ruber}$ and
429 temperature. The temperature influence on $\delta^{18}\text{O}_{ruber}$ was thus assessed by comparing the ambient temperature with the
430 $\delta^{18}\text{O}_{ruber}$ corrected for $\delta^{18}\text{O}_{sw}$ ($\delta^{18}\text{O}_{ruber} - \delta^{18}\text{O}_{sw}$). The pH of the seawater has also been identified as a factor affecting
431 the stable oxygen isotopic composition of planktic foraminifera (Bijma et al., 1999). However, as argued by Mulitza
432 et al., (2003), the limited modern surface seawater pH variability (Chakraborty et al., 2021) and its close dependence
433 on temperature implies that the pH contribution to $\delta^{18}\text{O}_{ruber}$ is well within the error associated with the measurements.
434 The seawater pH in the immediate vicinity of the foraminiferal shell is strongly influenced by the light intensity in the
435 presence of symbionts (Jorgensen et al., 1985). The riverine influx in the northern Indian Ocean makes the surface
436 waters turbid reducing the light penetration depths (Prasanna Kumar et al., 2010). Therefore, riverine influx induced
437 variations in turbidity in the northern Indian Ocean can influence the $\delta^{18}\text{O}_{ruber}$ via the pH effect.

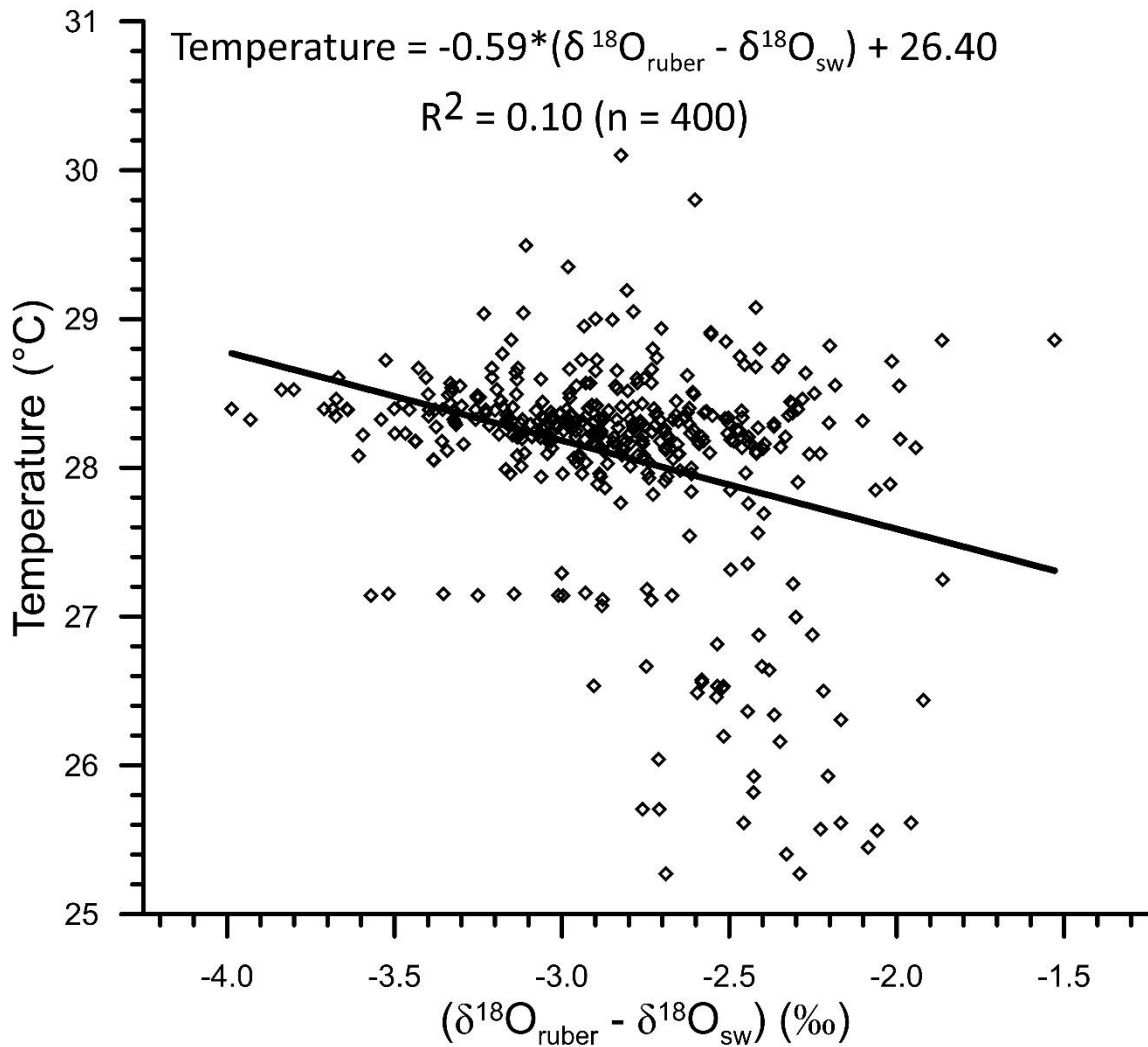
438 The comparison of $\delta^{18}\text{O}_{sw}$ corrected $\delta^{18}\text{O}_{ruber}$ with the ambient temperature also confirms the enrichment of
439 ($\delta^{18}\text{O}_{ruber} - \delta^{18}\text{O}_{sw}$) in heavier oxygen isotope with the decrease in temperature (Figure 13). We obtained the following
440 relationship between temperature and ($\delta^{18}\text{O}_{ruber} - \delta^{18}\text{O}_{sw}$) in the northern Indian Ocean.

441

$$442 \text{ Temperature} = -0.59 * (\delta^{18}\text{O}_{ruber} - \delta^{18}\text{O}_{sw}) + 26.40$$

443

444 The slope of the temperature and ($\delta^{18}\text{O}_{ruber} - \delta^{18}\text{O}_{sw}$) was somewhat different (0.17‰ per 1°C change in temperature)
445 than that of the temperature versus uncorrected $\delta^{18}\text{O}_{ruber}$, but similar as that reported for the plankton tows (0.22‰ per
446 1°C change in temperature) (Mulitza et al., 2003).



447
448

449 **Figure 13: The relationship between ambient temperature and $(\delta^{18}\text{O}_{\text{ruber}} - \delta^{18}\text{O}_{\text{sw}})$ for the northern Indian Ocean. As**
 450 **expected the $(\delta^{18}\text{O}_{\text{ruber}} - \delta^{18}\text{O}_{\text{sw}})$ gets enriched in heavier isotope with decreasing ambient temperature.**

451

452 7. Conclusions

453 We measured the stable oxygen isotopic ratio of the surface dwelling planktic foraminifera *Globigernoides ruber*
 454 white variety from the surface sediments of the northern Indian Ocean. A comparison of the $\delta^{18}\text{O}_{\text{ruber}}$ with the depth
 455 suggests a strong diagenetic alteration of the isotopic ratio. The fresh water influx induced changes in the ambient
 456 salinity exert the maximum influence on the $\delta^{18}\text{O}_{\text{ruber}}$ suggesting its robust application to reconstruct the past salinity
 457 in the northern Indian Ocean. The large east-west salinity gradient in the northern Indian Ocean results in a strong
 458 longitudinal variation in $\delta^{18}\text{O}_{\text{ruber}}$. The temperature influence on $\delta^{18}\text{O}_{\text{ruber}}$ is subdued as compared to the effect of large
 459 salinity variation in the northern Indian Ocean. We report a relatively smaller change in $\delta^{18}\text{O}_{\text{ruber}}$ with a unit increase

460 in ambient temperature in case of specimens retrieved from the surface sediments as compared to those collected live
461 from the water column.

462 **8. Data Availability**

463 The newly generated data as well as the data compiled from previous studies from the northern Indian Ocean has been
464 submitted to PANGAEA and is available at
465 <https://www.pangaea.de/tok/59190adf9e4facf7ebb9ad555c0bce58a9a72bd9> (Saraswat et al., 2022). The data is
466 submitted with the manuscript as well, for the reviewers' scrutiny.

467 **9. Author Contribution**

468 RS designed the research, compiled and interpreted the data and wrote the manuscript. TS, DKN, DPS, SMS, MS,
469 GS, SRB, SRK picked the specimens for isotopic analysis. MM, ASM supervised the analysis. All authors edited and
470 contributed to the final manuscript.

471 **10. Competing Interests**

472 The authors declare that they have no conflict of interest.

473 **Acknowledgements**

474 We thank the crew onboard expeditions during which the surface sediment samples were collected. The authors thank
475 the Director, CSIR-National Institute of Oceanography for the facilities and funding. The technical personnel at the
476 Alfred-Wegener Institute for Polar and Marine Research, and MARUM, Bremen University, Germany, are
477 acknowledged for the help in stable isotopic analysis. We thank Dr. P.S. Rao and Dr. V. Ramaswamy, CSIR-NIO for
478 providing the surface sediment samples collected from the Myanmar continental shelf. The authors also thank Dr.
479 B.N. Nath for providing the spade core-top samples from the eastern margin of India. We thank Dr. Alberto Sanchez,
480 Centro Interdisciplinario de Ciencias Marinas, Instituto Politécnico Nacional, La Paz, B.C.S, Mexico, and the
481 anonymous reviewer, for their constructive comments and suggestions that helped to improve the manuscript.

482

483

484 **References**

- 485
- 486 Achyuthan, H., Deshpande, R.D., Rao, M.S., Kumar, B., Nallathambi, T., Shashi Kumar, K., Ramesh, R.,
487 Ramachandran, P., Maurya, A.S., and Gupta, S.K.: Stable isotopes and salinity in the surface waters of the Bay of
488 Bengal: Implications for water dynamics and palaeoclimate. *Mar. Chem.*, 149, 51-62, 2013.
- 489 Anderson, D.M.: Attenuation of millennial-scale events by bioturbation in marine sediments. *Paleoceanography*, 16,
490 352–357, 2001.
- 491 Bé, A.W.H., and Hutson, W.H.: Ecology of planktonic foraminifera and biogeographic patterns of life and fossil
492 assemblages in the Indian Ocean. *Micropaleontology*, 23, 369, 1977.
- 493 Bemis, B.E., Spero, H.J., Bijma, J., and Lea, D.W.: Reevaluation of the oxygen isotopic composition of planktonic
494 foraminifera: Experimental results and revised paleotemperature equations. *Paleoceanography* 13, 150-160, 1998.
- 495 Berger, W.H.: Sedimentation of planktonic foraminifera. *Mar. Geol.*, 11, 325-358, 1971.
- 496 Berger, W.H., and Killingley, J.S.: Glacial-Holocene transition in deep-sea carbonates: selective dissolution and the
497 stable isotope signal. *Science*, 197, 563-566, 1977.
- 498 Bhadra, S.R., and Saraswat, R.: Assessing the effect of riverine discharge on planktic foraminifera: A case study from
499 the marginal marine regions of the western Bay of Bengal. *Deep Sea Res. II: Topical Stud. Oceanogra.*, 183,
500 104927, 2021.
- 501 Bhattacharya, S.K., Gupta, S.K. and Krishnamurthy, R.V.: Oxygen and hydrogen isotopic ratios in ground waters and
502 river waters from India. *Proc. Indian Acad. Sci. (Earth Planet. Sci.)*, 94, 283-295, 1985.
- 503 Bhonsale, S., and Saraswat, R.: Abundance and size variation of *Globorotalia menardii* in the northeastern Indian
504 Ocean during the late Quaternary. *J. Geol. Soc. India*, 80, 771-782, 2012.
- 505 Bijma, J., Spero, H.J., and Lea, D.W.: Reassessing foraminiferal stable isotope geochemistry: Impact of the oceanic
506 carbonate system (experimental results). In: Fischer, G., Wefer, G. (Eds.), *Use of Proxies in Paleoclimatology:
507 Examples from the South Atlantic*. Springer, Berlin, pp. 489-512, 1999.
- 508 Bonneau, M.-C., Vergnaud-Grazzini, C., and Berger, W.H.: Stable isotope fractionation and differential dissolution
509 in Recent planktonic foraminifera from Pacific box-cores. *Oceanologica Acta*, 3, 377-382, 1980.
- 510 Boyer, T. P., Antonov, J. I., Baranova, O. K., Garcia, H. E., Johnson, D. R., Mishonov, A. V., et al.: *World Ocean
511 Database*, 2013.
- 512 Bristow, L.A., Callbeck, C.M., Larsen, M., Altabet, M.A., Dekazemacker, J., Forth, M., Gauns, M., Glud, R.N.,
513 Kuypers, M.M.M., Lavik, G., Milucka, J., Naqvi, S.W. A., Pratihary, A., Revsbech, N. P., Thamdrup, B., Treusch,
514 A.H., and Canfield, D. E.: N₂ production rates limited by nitrite availability in the Bay of Bengal oxygen minimum
515 zone. *Nat. Geosci.*, 10, 24-29, 2017.
- 516 Broecker, W.S.: Oxygen isotope constraints on surface ocean temperatures. *Quat. Res.*, 26, 121–134,
517 [https://doi.org/10.1016/0033-5894\(86\)90087-6](https://doi.org/10.1016/0033-5894(86)90087-6), 1986.
- 518 Chaitanya, A.V.S., Lengaigne, M., Vialard, J., Gopalakrishna, V.V., Durand, F., Kranthikumar, C., Amritash, S.,
519 Suneel, V., Papa, F., and Ravichandran, M.: Salinity measurements collected by fishermen reveal a “river in the
520 sea” flowing along the eastern coast of India. *Bull. American Met. Soc.*, 95, 1897-1908, 2014.

521 Chakraborty, K., Valsala, V., Bhattacharya, T., and Ghosh, J.: Seasonal cycle of surface ocean pCO₂ and pH in the
522 northern Indian Ocean and their controlling factors. *Progr. Oceanogra.*, 198, 102683, 2021.

523 Chatterjee, A., Kumar, B.P., Prakash, S., and Singh, P.: Annihilation of the Somali upwelling system during summer
524 monsoon. *Sci. Rep.*, 9, 1-14, 2019.

525 Dämmer, L.K., de Nooijer, L., van Sebille, E., Haak, J.G., and Reichert, G.-J.: Evaluation of oxygen isotopes and
526 trace elements in planktonic foraminifera from the Mediterranean Sea as recorders of seawater oxygen isotopes
527 and salinity. *Clim. Past*, 16, 2401-2414, 2020.

528 De Deckker, P.: The Indo-Pacific Warm Pool: critical to world oceanography and world climate. *Geosci. Lett.*, 3, 20,
529 2016.

530 Delaygue, G., Bard, E., Rollion, C., Jouzel, J., Stievenard, M., and Duplessy, J.-C.: Oxygen isotope/salinity
531 relationship in the northern Indian Ocean. *J. Geophys. Res.*, 106, 4565-4574, 2001.

532 Delaygue, G., J. Jouzel, and Dutay, J.C.: Oxygen 18–salinity relationship simulated by an oceanic general circulation
533 model. *Earth Planet. Sci. Lett.*, 178, 113-123, 2000.

534 Duplessy, J.C., Bé, A.W.H., and Blanc, P.L.: Oxygen and carbon isotopic composition and biogeographic distribution
535 of planktonic foraminifera in the Indian Ocean. *Palaeogeogra., Palaeoclimatol., Palaeoecol.*, 33, 9-46, 1981.

536 Duplessy, J.C.: Glacial to interglacial contrasts in the northern Indian Ocean. *Nature*, 295, 494-498, 1982.

537 Duplessy, J.C., Blanc, P.L., and Bé, A.W.H.: Oxygen-18 enrichment of planktonic foraminifera due to gametogenic
538 calcification below the euphotic zone. *Science*, 213, 1247-1250, 1981.

539 Emiliani, C.: Depth habitat of some species of pelagic foraminifera as indicated by oxygen isotope ratio. *American J.*
540 *Sci.*, 252, 149-158, 1954.

541 Erez, J., and Luz, B.: Experimental paleotemperature equation for planktonic foraminifera. *Geochim. Cosmochim.*
542 *Acta*, 47, 1025-1031, 1983.

543 Fairbanks, R. G. and Wiebe, P. H.: Foraminifera and chlorophyll maximum: vertical distribution, seasonal succession,
544 and paleoceanographic significance, *Science (New York, N.Y.)*, 209, 1524–1526,
545 <https://doi.org/10.1126/science.209.4464.1524>, 1980.

546 Fraile, I., Schulz, M., Mulitza, S., and Kucera, M.: Predicting the global distribution of planktonic foraminifera using
547 a dynamic ecosystem model. *Biogeosciences*, 5, 891-911, 2008.

548 Ganssen, G., and Kroon, D.: Evidence for Red Sea surface water circulation from oxygen isotopes of modern surface
549 waters and planktonic foraminiferal tests. *Paleoceanography*, 6, 73-82, 1991.

550 Gerino, M., Aller, R.C., Lee, C., Cochran, J.K., Aller, J.Y., Green, M.A. and Hirschberg, D.: Comparison of different
551 tracers and methods used to quantify bioturbation during a spring bloom: 234-Thorium, luminophores and
552 chlorophyll a. *Estuarine Coast. Shelf Sci.*, 46, 531–547, 1998.

553 Guptha, M.V.S., Curry, W.B., Ittekkot, V., and Muralinath, A.S.: Seasonal variation in the flux of planktic
554 foraminifera: Sediment trap results from the Bay of Bengal, northern Indian Ocean. *J. Foraminiferal Res.*, 27, 5-
555 19, 1997.

556 Hemleben, C., Spindler, M., and Anderson, O. R.: *Modern Planktonic Foraminifera*, Springer-Verlag, New York,
557 1989.

558 Hollstein, M., Mohtadi, M., Rosenthal, Y., Moffa Sanchez, P., Oppo, D., Martínez Méndez, G., Steinke, S., and
559 Hebbeln, D.: Stable oxygen isotopes and Mg/Ca in planktic foraminifera from modern surface sediments of the
560 Western Pacific Warm Pool: Implications for thermocline reconstructions. *Paleoceanography*, 32, 1174-1194,
561 2017.

562 Horikawa, K., Kodaira, T., Zhang, J., and Murayama, M.: $\delta^{18}\text{O}_{\text{sw}}$ estimate for *Globigerinoides ruber* from core-top
563 sediments in the East China Sea. *Progr. Earth Planet. Sci.*, 2, 19, 2015.

564 Howden, S. D., and Murtugudde, R.: Effects of river inputs into the Bay of Bengal. *J. Geophys. Res.*, 106(C9), 19825-
565 19844, 2001.

566 Hut, G.: Consultants group meeting on stable isotope reference samples for geochemical and hydrological
567 investigations. Report to the Director General, International Atomic Energy Agency, Vienna, 42 pp, 1987.

568 Jørgensen, B. B., Erez, J., Revsbech, P., and Cohen, Y.: Symbiotic photosynthesis in a planktonic foraminiferan,
569 *Globigerinoides sacculifer* (Brady), studied with microelectrodes. *Limnol. Oceanogr.*, 30, 1253–1267, 1985.

570 Joseph, S., and Freeland, H.J.: Salinity variability in the Arabian Sea. *Geophys. Res. Lett.*, 32, L09607, 2005.

571 Kallel, N., Paterne, M., Duplessy, J., Vergnaudgrazzini, C., Pujol, C., Labeyrie, L., Arnold, M., Fontugne, M., and
572 Pierre, C.: Enhanced rainfall in the Mediterranean region during the last Sapropel Event. *Oceanologica Acta*, 20,
573 1997.

574 Kathayat, G., Sinha, A., Tanoue, M., K. Yoshimura, H. Li, Zhang, H., and Cheng, H.: Interannual oxygen isotope
575 variability in Indian summer monsoon precipitation reflects changes in moisture sources. *Comm. Earth Environ.*,
576 2, 96, 2021.

577 Kemle-von-Mücke, S., and Hemleben, C.: Planktic Foraminifera. In: Boltovskoy E (ed) South Atlantic zooplankton.
578 Backhuys Publishers, Leiden, pp 43-67, 1999.

579 Kessarkar, P.M., Purnachandra Rao, V., Naqvi, S.W.A., and Karapurkar, S.G.: Variation in the Indian summer monsoon
580 intensity during the Bølling-Ållerød and Holocene. *Paleoceanography*, 28, 413-425, 2013.

581 Kim, S.T., and O'Neil, J.R.: Equilibrium and nonequilibrium oxygen isotope effects in synthetic carbonates. *Geochim.*
582 *Cosmochim. Acta*, 61, 3461-3475, 1997.

583 Kroon, D., and Ganssen, G.: Northern Indian Ocean upwelling cells and the stable isotope composition of living
584 planktonic foraminifers. *Deep-Sea Res.*, 36, 1219-1236, 1989.

585 Kumar, B., S. P. Rai, U. Saravana Kumar, S. K. Verma, P. Garg, S. V. Vijaya Kumar, R. Jaiswal, B. K. Purendra, S.
586 R. Kumar, and N.G. Pande: Isotopic characteristics of Indian precipitation. *Water Resource Res.*, 46, W12548,
587 2010.

588 Lambeck, K., H. Rouby, A. Purcell, Y. Sun, and M. Sambridge: Sea level and global ice volumes from the Last Glacial
589 Maximum to the Holocene. *Proc. Nat. Acad. Sci.*, 111, 15296–15303, 2014.

590 Lea, D.W.: Elemental and isotopic proxies of past ocean temperatures. *Treatise Geochem.*, 8, 373-397, 2014.

591 Locarnini, R. A., Mishonov, A. V., Baranova, O. K., Boyer, T. P., Zweng, M. M., Garcia, H. E., Reagan, J. R., Seidov,
592 D., Weathers, K., Paver, C. R. and Smolyar, I.: World Ocean Atlas 2018, Volume 1: Temperature. A. Mishonov
593 Technical Ed.; NOAA Atlas NESDIS 81, 52pp, 2018.

594 Lohmann, G. P.: A model for variation in the chemistry of planktonic foraminifera due to secondary calcification and
595 selective dissolution. *Paleoceanography*, 10, 445-457, 1995.

596 Löwemark, L., and Grootes, P.M.: Large age differences between planktic foraminifers caused by abundance
597 variations and Zoophycos bioturbation. *Paleoceanography*, 19, PA2001, doi:10.1029/2003PA000949, 2004.

598 Löwemark, L., Hong, W.-L., Yui, T.-F., and Hung, G.-W.: A test of different factors influencing the isotopic signal
599 of planktonic foraminifera in surface sediments from the northern South China Sea. *Mar. Micropaleontol.* 55, 49-
600 62, 2005.

601 Madhu, N.V., Jyothibabu, R., Maheswaran, P.A., Gerson, V.J., Gopalakrishnan, T.C., and Nair, K.K.C.: Lack of
602 seasonality in phytoplankton standing stock (chlorophyll a) and production in the western Bay of Bengal. *Cont.*
603 *Shelf Res.*, 26, 1868-1883, 2006.

604 Madhupratap, M., S.P. Kumar, P.M.A. Bhattathiri, M.D. Kumar, S. Raghukumar, K.K.C. Nair, and N. Ramaiah:
605 Mechanism of the biological response to winter cooling in the northeastern Arabian Sea. *Nature*, 384, 549-552,
606 1996.

607 Mahesh, B.S., and Banakar, V.K.: Change in the intensity of low-salinity water inflow from the Bay of Bengal into
608 the Eastern Arabian Sea from the Last Glacial Maximum to the Holocene: Implications for monsoon variations.
609 *Palaeogeogra., Palaeoclimatol., Palaeoecol.*, 397, 31-37, 2014.

610 McCorkle, D. C., Martin, P. A., Lea, D. W., and Klinkhammer, G.P.: Evidence of a dissolution effect on benthic
611 foraminiferal shell chemistry: $\delta^{13}\text{C}$, Cd/Ca, Ba/Ca, and Sr/Ca results from the Ontong Java Plateau.
612 *Paleoceanography*, 10, 699-714, 1997.

613 Metcalfe, B., Feldmeijer, W., and Ganssen, G.M.: Oxygen isotope variability of planktonic foraminifera provide clues
614 to past upper ocean seasonal variability. *Paleoceanogra. Paleoclimatol.*, 34, 374–393, 2019.

615 Mohtadi, M., Oppo, D.W., Lückge, A., DePol-Holz, R., Steinke, S., Groeneveld, J., Hemme, N., and Hebbeln, D.:
616 Reconstructing the thermal structure of the upper ocean: Insights from planktic foraminifera shell chemistry and
617 alkenones in modern sediments of the tropical eastern Indian Ocean. *Paleoceanography*, 26, PA3219, 2011.

618 Mulitza, S., Boltovskoy, D., Donner, B., Meggers, H., Paul, A., and Wefer, G.: Temperature: $\delta^{18}\text{O}$ relationships of
619 planktonic foraminifera collected from surface waters. *Palaeogeogra., Palaeoclimatol., Palaeoecol.*, 202, 143-152,
620 2003.

621 Mulitza, S., Dürkoop, A., Hale, W., Wefer, G., and Niebler, H.S.: Planktonic foraminifera as recorders of past surface-
622 water stratification. *Geology*, 25, 335-338, 1997.

623 Mulitza, S., Wolff, T., Pätzold, J., Hale, W., and Wefer, G.: Temperature sensitivity of planktic foraminifera and its
624 influence on the oxygen isotope record. *Mar. Micropaleontol.*, 33, 223-240, 1998.

625 Naqvi, S.W.A.: Deoxygenation in marginal seas of the Indian Ocean. *Front. Mar. Sci.*, 8, 624322. doi:
626 10.3389/fmars.2021.624322, 2021.

627 Naqvi, S.W.A., H. Naik, A. Pratihary, W. D'souza, P.V. Narvekar, D.A. Jayakumar, A.H. Devol, T. Yoshinari, and T.
628 Saino: Coastal versus open-ocean denitrification in the Arabian Sea. *Biogeosciences*, 3, 621-633, 2006.

629 Panchang, R., and Nigam, R.: High resolution climatic records of the past~ 489 years from Central Asia as derived
630 from benthic foraminiferal species, *Asterorotalia trispinosa*. *Mar. Geol.*, 307, 88-104, 2012.

631 Pearson, P.N.: Oxygen isotopes in foraminifera: Overview and historical review. In *Reconstructing Earth's Deep-*
632 *Time Climate—The State of the Art in 2012*, Paleontological Society Short Course, November 3, 2012. The
633 Paleontological Society Papers, Volume 18, Linda C. Ivany and Brian T. Huber (eds.), pp. 1-38, 2012.

634 Prasanna Kumar, S., J. Narvekar, M. Nuncio, M. Gauns, and S. Sardesai: What drives the biological productivity of
635 the northern Indian Ocean? *Washington DC American Geophysical Union Geophysical Monograph Series*, 185,
636 33-56, 2009.

637 Prasanna Kumar, S., Narvekar, J., Nuncio, M., Kumar, A., Ramaiah, N., Sardesai, S., Gauns, M., Fernandes, V., and
638 Paul J.: Is the biological productivity in the Bay of Bengal light limited? *Curr. Sci.*, 98, 1331-1339, 2010.

639 Prasanna Kumar, S., M. Nuncio, J. Narvekar, A. Kumar, D.S. Sardesai, S.N. De Souza, M. Gauns, N. Ramaiah, and
640 M. Madhupratap: Are eddies nature's trigger to enhance biological productivity in the Bay of Bengal? *Geophys.*
641 *Res. Lett.*, 31, L07309, doi:10.1029/2003GL019274, 2004.

642 Prasanna Kumar, S., and Prasad, T.G.: Formation and spreading of Arabian Sea high-salinity water mass. *J. Geophys.*
643 *Res: Oceans*, 104, 1455-1464, 1999.

644 Prell, W.L., and Curry, W.B.: Faunal and isotopic indices of monsoonal upwelling: Western Arabian Sea.
645 *Oceanologica Acta*, 4, 91-98, 1981.

646 Qasim, S.Z.: Biological productivity of the Indian Ocean. *Indian J. Mar. Sci.*, 6, 122–137, 1977.

647 Rai, S.P., J. Noble, D. Singh, Y.S. Rawat, and B. Kumar: Spatiotemporal variability in stable isotopes of the Ganga
648 River and factors affecting their distributions. *Catena*, 204, 105360, 2021.

649 Ramaswamy, V., Gaye, B., Shirodkar, P.V., Rao, P.S., Chivas, A. R., Wheeler, D., and Thwin, S.: Distribution and
650 sources of organic carbon, nitrogen and their isotopic signatures in sediments from the Ayeyarwady (Irrawaddy)
651 continental shelf, northern Andaman Sea. *Mar. Chem.*, 111, 137-150, 2008.

652 Ramesh, R. and Sarin, M.M.: Stable isotope study of the Ganga (Ganges) river system. *J. Hydrology*, 139, 49-62,
653 1992.

654 Rao, R. R., and Sivakumar, R.: Seasonal variability of sea surface salinity and salt budget of the mixed layer of the
655 northIndian Ocean. *J. Geophys. Res.*, 108(C1), 3009, 2003.

656 Rixen, T., Cowie, G., Gaye, B., Goes, J., do Rosário Gomes, H., Hood, R.R., Lachkar, Z., Schmidt, H., Segsneider,
657 J., and Singh, A.: Reviews and syntheses: Present, past, and future of the oxygen minimum zone in the northern
658 Indian Ocean. *Biogeosciences*, 17, 6051-6080, 2020.

659 Rochford, D. J.: Salinity maximum in the upper 100 meters of the north Indian Ocean. *Aust. J. Mar. Freshwater Res.*,
660 15, 1-24, 1964.

661 Rozanski, K., Araguás-Araguás, L., and Gonfiantini, R.: Isotopic Patterns in Modern Global Precipitation, in: *Climate*
662 *Change in Continental Isotopic Records*, edited by: Swart, P. K., Lohmann, K. C., Mckenzie, J., and Savin, S.,
663 American Geophysical Union, Washington, D. C., 1–36, <https://doi.org/10.1029/GM078p0001>, 1993.

664 Saalim, S.M., Saraswat, R., and Nigam, R.: Ecological preferences of living benthic foraminifera from the Mahanadi
665 river-dominated north-western Bay of Bengal: A potential environmental impact assessment tool. *Mar. Poll. Bull.*,
666 175, 113158, 2022.

667 Sánchez, A., Sánchez-Vargas, L., Balart, E., and Domínguez-Samalea, Y.: Stable oxygen isotopes in planktonic
668 foraminifera from surface sediments in the California Current system. *Mar. Micropaleontol.*, 173, 102127, 2022.

669 Saraswat, R., Lea, D.W., Nigam, R., Mackensen, A., and Naik, D.K.: Deglaciation in the tropical Indian Ocean driven
670 by interplay between the regional monsoon and global teleconnections. *Earth Planet. Sci. Lett.*, 375, 166-175,
671 2013.

672 Saraswat, R., Nigam, R., Mackensen, A., and Weldeab, S.: Linkage between seasonal insolation gradient in the tropical
673 northern hemisphere and the sea surface salinity of the equatorial Indian Ocean during the last glacial period. *Acta*
674 *Geol. Sinica*, 86, 801–811, 2012.

675 Saraswat, R., Singh, D.P., Lea, D.W., Mackensen, A., and Naik, D.K.: Indonesian throughflow controlled the
676 westward extent of the Indo-Pacific Warm Pool during glacial-interglacial intervals. *Global Planet. Cha.*, 183,
677 103031, 2019.

678 Saraswat, R., Suokhrie, T., Naik, D.K., Singh, D.P., Saalim, S.M., Salman, M., Kumar, G., Bhadra, S.R., Mohtadi,
679 M., Kurtarkar, S.R., and Maurya, A.S.: Oxygen isotopic ratio of *Globigerinoides ruber* (white variety) in the
680 surface sediments of the northern Indian Ocean. PANGAEA, <https://doi.org/10.1594/PANGAEA.945401>, 2022.

681 Sarma, V.V. and Aswanikumar, V.: Subsurface chlorophyll maxima in the north-western Bay of Bengal. *J. Plankton*
682 *Res.*, 11, 339-352, 1991.

683 Sarma, V.V.S.S., Chopra, M., Rao, D.N., Priya, M.M.R., Rajula, G.R., Lakshmi, D.S.R., and Rao, V.D.: Role of
684 eddies on controlling total and size-fractionated primary production in the Bay of Bengal. *Cont. Shelf Res.*, 204,
685 104186, 2020.

686 Schlitzer, R., Ocean Data View, <https://odv.awi.de>, 2018.

687 Schmidt, G.A., Bigg, G.R., and Rohling, E.J.: "Global Seawater Oxygen-18 Database - v1.22"
688 <https://data.giss.nasa.gov/o18data/>, 1999.

689 Schmidt, M.W., Spero, H.J., and Lea, D.W.: Links between salinity variation in the Caribbean and North Atlantic
690 thermohaline circulation. *Nature*, 428, 160–163, 2004.

691 Schrag, D.P., DePaolo, D.J., Richter, F.M.: Reconstructing past sea surface temperatures: Correcting for diagenesis
692 of bulk marine carbonate. *Geochim. Cosmochim. Acta*, 59, 2265–2278, 1995.

693 Sengupta, D., Bharath Raj, G.N., and Shenoi, S.S.C.: Surface freshwater from Bay of Bengal runoff and Indonesian
694 Throughflow in the tropical Indian Ocean. *Geophys. Res. Lett.*, 33, L22609, 2006.

695 Shackleton, N.J.: Oxygen isotopes, ice volume and sea level. *Quat. Sci. Rev.*, 6, 183-190, 1987.

696 Shackleton, N.J.: The 100,000-year Ice-Age cycle identified and found to lag temperature, carbon dioxide, and orbital
697 eccentricity. *Science*, 289, 1897-1902, 2000.

698 Shackleton, N.J., and Vincent, E.: Oxygen and carbon isotope studies in recent foraminifera from the southwest Indian
699 ocean. *Mar. Micropaleontol.*, 3, 1-13, 1978.

700 Shankar, D., Vinayachandran, P.N., and Unnikrishnan, A.S.: The monsoon currents in the north Indian Ocean. *Progr.*
701 *Oceanogra.*, 52, 63–120, 2002.

702 Shetye, S.R., Gouveia, A.D., and Shenoi, S.S.C.: Circulation and water masses of the Arabian Sea. *Proc. Indian Acad.*
703 *Sci. (Earth Planet. Sci.)*, 103, 107-123, 1994.

704 Shetye, S.R., Shenoi, S.S.C., Gouveia, A.D., Michael, G.S., Sundar, D., and Nampoothiri, G.: Wind-driven coastal
705 upwelling along the western boundary of the Bay of Bengal during the southwest monsoon. *Cont. Shelf Res.*, 11,
706 1397-1408, 1991.

707 Singh, A., Jani, R.A., and Ramesh, R.: Spatiotemporal variations of the $\delta^{18}\text{O}$ -salinity relation in the northern Indian
708 Ocean. *Deep-Sea Res. I*, 57, 1422-1431, 2010.

709 Singh, D.P., Saraswat, R., and Naik, D.K.: Does glacial-interglacial transition affect sediment accumulation in
710 monsoon dominated regions? *Acta Geol. Sinica*, 91, 1079-1094, 2017.

711 Singh, D.P., Saraswat, R., and Nigam, R.: Untangling the effect of organic matter and dissolved oxygen on living
712 benthic foraminifera in the southeastern Arabian Sea. *Mar. Poll. Bull.*, 172, 112883, 2021.

713 Sirocko, F.: Zur Akkumulation von Staubsedimenten im nördlichen Indischen Ozean; Anzeiger der Klimageschichte
714 Arabiens und Indiens. Dissertation, Berichte-Reports, Geologisch-Paläontologisches Institut der Universität Kiel,
715 27, 185 pp, 1989.

716 Smitha, A., Joseph, K.A., Jayaram, C., and Balchand, A.N.: Upwelling in the southeastern Arabian Sea as evidenced
717 by Ekman mass transport using wind observations from OCEANSAT-II Scatterometer. *Indian J. Geo-mar. Sci.*,
718 43, 111-116, 2014.

719 Spero, H.J., Bijma, J., Lea, D.W., and Bemis, B.B.: Effect of seawater carbonate concentration on foraminiferal carbon
720 and oxygen isotopes. *Nature*, 390, 497-500, 1997.

721 Sridevi, B., and Sarma, V.V.S.S.: A revisit to the regulation of oxygen minimum zone in the Bay of Bengal. *J. Earth
722 Syst. Sci.*, 129, 1-7, 2020.

723 Stainbank, S., Kroon, D., Rüggeberg, A., Raddatz, J., de Leau, E.S., Zhang, M., et al.: Controls on planktonic
724 foraminifera apparent calcification depths for the northern equatorial Indian Ocean. *PLoS ONE* 14, e0222299,
725 2019.

726 Suokhrie, T., Saraswat, R., and Nigam, R.: Multiple ecological parameters affect living benthic foraminifera in the
727 river-influenced west-central Bay of Bengal. *Front. Mar. Sci.*, 8, 467, 2021a.

728 Suokhrie, T., Saraswat, and R., Saju, S.: Strong solar influence on multi-decadal periodic productivity changes in the
729 central-western Bay of Bengal. *Quat. Int.*, <https://doi.org/10.1016/j.quaint.2021.04.015>, 2021b.

730 Thirumalai, K., Richey, J.N., Quinn, T.M., and Poore, R.Z.: *Globigerinoides ruber* morphotypes in the Gulf of
731 Mexico: A test of null hypothesis. *Sci. Rep.*, 4, 6018, 2014.

732 Thompson, P.R., Bé, A.W.H., Duplessy, J.-C., and Shackleton, N.J.: Disappearance of pink-pigmented
733 *Globigerinoides ruber* at 120,000 yr BP in the Indian and Pacific oceans. *Nature*, 280, 554-558, 1979.

734 Thunell, R., Tappa, E., Pride, C., and Kincaid, E.: Sea-surface temperature anomalies associated with the 1997-1998
735 El Niño recorded in the oxygen isotope composition of planktonic foraminifera. *Geology*, 27, 843,
736 [https://doi.org/10.1130/0091-7613\(1999\)027<0843:SSTAAW>2.3.CO;2](https://doi.org/10.1130/0091-7613(1999)027<0843:SSTAAW>2.3.CO;2), 1999.

737 Tiwari, M., Nagoji, S.S., Kartik, T., Drishya, G., Parvathy, R.K., and Rajan, S.: Oxygen isotope-salinity relationships
738 of discrete oceanic regions from India to Antarctica vis-à-vis surface hydrological processes. *J. Mar. Syst.*, 113-
739 114, 88-93, 2013.

740 Urey, H.C.: The thermodynamic properties of isotopic substances. *J. Chem. Soc.*, 12, 562-569, 1947.

741 Vergnaud-Grazzini, C.: Non-equilibrium isotopic compositions of shells of planktonic foraminifera in the
742 Mediterranean Sea. *Palaeogeogra., Palaeoclimatol., Palaeoecol.*, 20, 263-276, 1976.

743 Vinayachandran, P.N., and Shetye, S.R.: The warm pool in the Indian Ocean. *Proc. Indian Acad. Sci. (Earth Planet*
744 *Sci.)* 100, 165-175, 1991.

745 Waelbroeck, C., Mulitza, S., Spero, H., Dokken, T., Kiefer, T., and Cortijo, E.: A global compilation of late Holocene
746 planktonic foraminiferal $\delta^{18}\text{O}$: relationship between surface water temperature and $\delta^{18}\text{O}$. *Quat. Sci. Rev.*, 24, 853–
747 868, <https://doi.org/10.1016/j.quascirev.2003.10.014>, 2005.

748 Wang, L., Sarnthein, M., Duplessy, J.-C., Erlenkeuser, H., Jung, S., and Pflaumann, U.: Paleo sea surface salinities in
749 the low-latitude Atlantic: The $\delta^{18}\text{O}$ record of *Globigerinoides ruber* (white). *Paleoceanography*, 10, 749-761, 1995.

750 Wu, G., and Berger, W.H.: Planktonic foraminifera: differential dissolution and the quaternary stable isotope record
751 in the west equatorial Pacific. *Paleoceanography*, 4, 181-198, 1989.

752 Wycech, J.B., Kelly, D.C., Kitajima, K., Kozdon, R., Orland, I.J., and Valley, J.W.: Combined effects of gametogenic
753 calcification and dissolution on $\delta^{18}\text{O}$ measurements of the planktic foraminifer *Trilobatus sacculifer*. *Geochem.*
754 *Geophys. Geosys.*, 19, <https://doi.org/10.1029/2018GC007908>, 2018.

755 Zweng, M M., Reagan, J. R., Seidov, D., Boyer, T. P., Locarnini, R. A., Garcia, H. E., Mishonov, A. V., Baranova,
756 O. K., Weathers, K., Paver, C. R. and Smolyar, I.: World Ocean Atlas 2018, Volume 2: Salinity. A. Mishonov
757 Technical Ed.; NOAA Atlas NESDIS 82, 50pp, 2018.